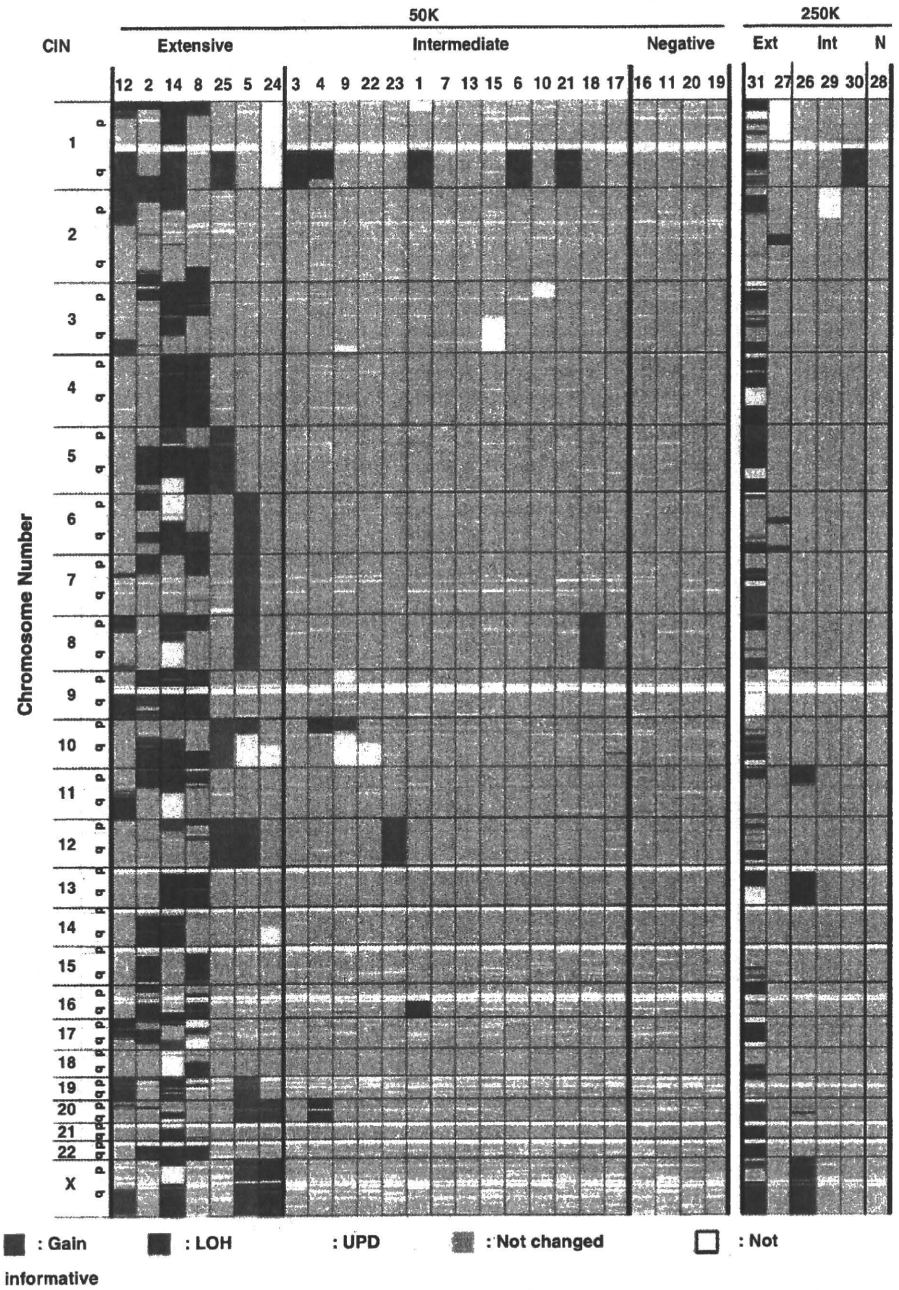

Figure 1 Overview of genomic imbalance in endometrial carcinomas. SNP array was performed in 31 clinical samples with paired tumor DNA and normal DNA, using a human mapping 50K or 250K Array. Samples are categorized according to the level of chromosomal instability (CIN) as described in the text; CIN-extensive (Ext) with five or more copy number changes, CIN-intermediate (Int) with 1–4 copy number changes, and CIN-negative (N) without any copy number changes.

We detected five HD candidate regions in three samples. One of the five regions (6q21.2) was located in the vicinity of a known CNV. Genome imbalance map (GIM) algorithm using the control DNA in this sample with the other from unrelated individuals revealed hemizygous loss at the surrounding region in the germline DNA, suggesting that this locus is not somatic HD. The other four HD regions on 9p21.3, 10q23.3, 11p15.1 and 17q11.21 did not match with any known CNVs and included *CDKN2A*, *CDKN2B*, *ELAVL2*, *PTEN*, *NELL1*, *IDH3GL* and *NF1* genes. All these regions were <4.2 Mb and were included in the LOH regions (Figure 1 and Supplementary Table 3).

SNP array genotyping distinguishes three clusters according to the degree of CIN

As the number of copy alterations is significantly different in each tumor, we further divided the CIN-positive tumors into CIN-extensive and CIN-intermedi-

Table 1 Minimal regions of copy number neutral (CNN) LOH in endometrial carcinomas

SNP probes	*Sample#*	*Chromosome/ cytoband*	*Start*	*End*	*Minimal region (Mb)*	*Cancer-related genes*
	1	1p36.32–1p36.11	3 464 664	24 689 967	21.225303	*MDS2, SDHB, PAX7, RPL22*
	2	11p13	34 400 995	34 569 744	0.168749	
		14q24.1	66 751 027	67 553 008	0.801981	*RAD51L1*
	5	10q11.23–10q26.3*	49 154 970	132 221 295	83.066325	*BMPR1A, NCOA, D10S170, LCX, PRF1, MYST4, PTEN, NFKB2, TLX1, TNFRSF6, SUFU, FGFR2*
	8	3p14.2–3p14.1	61 464 727	64 834 115	3.369388	
		6q23.2	134 231 263	134 325 485	0.094222	
		7p15.2	25 504 107	25 728 845	0.224738	
		9p22.3	15 722 332	15 750 822	0.02849	
		11p15.4	2 861 092	8 302 275	5.441183	*LMO1, NUP98*
		12q13.13	50 605 518	51 445 539	0.840021	
		17p13.3–17p11.2	489 977	22 269 537	21.77956	*GAS7, BHD, HCMOGT-1, MAP2K4, RAB5EP, TP53, USP6*
		17q21.31–17q21.32	42 127 241	46 355 386	4.228145	
		17q21.33–17q25.3	48 767 363	81 267 388	32.500025	*DDX5, BRIP1, HLF, MSI2, PRKAR1A, ASPSCR1, CANT1, ALO17, MSF*
	9	3q26.31–3q29	176 959 377	198 389 829	21.430452	*PIK3CA, BCL6, EIF4A2, ETV5, LPP, TFRC*
		9p24.3–9p13.3	239 391	35 436 386	35.196995	*FANCG, CDKN2A- p14ARF, CDKN2A -p16(INK4a), MLLT3, PSIP2, JAK2*
50K		10q11.21–10q26.3*	43 685 003	134 750 136	91.065133	*BMPR1A, NCOA4, D10S170, LCX, PRF1, MYST4, PTEN, NFKB2, TLX1, TNFRSF6, SUFU, FGFR2*
	10	3p26.3–3p21.33	394 143	43 747 869	43.353726	*PPARG, MLH1, CTNNB1, RAF1, VHL, XPC, SRGAP3, FANCD2*
	14	5q31.1–5q35.3	135 051 159	180 180 911	45.129752	*GRAF, ITK, PDGFRB, CD74, RANBP17, NPM1, NSD1, TLX3*
		6p	Whole arm	Whole arm	Whole arm	*HSPCB, CCND3, HMGA1, SFRS3, TFEB, PIM1, HIST1H4I, POU5F1, FANCE, TRIM27, DEK*
		6q11.1–6q14.1	62 019 084	78 728 757	16.709673	
		8q13.1–8q24.23	67 274 844	137 516 772	70.241928	*NCOA2, NBS1, CBFA2T1, COX6C, EXT1, MYC*
		11q13.1–11q25	64 820 346	134 034 111	69.213765	*NUMA1, CCND1, PICALM, ATM, BIRC3, MAML2, DDX10, PAFAH1B2, MLL, SDHD, POU2AF1, ZNF145, CBL, DDX6, PCSK7, ARHGEF12, FLI1*
		18p	Whole arm	Whole arm	Whole arm	
		18q	Whole arm	Whole arm	Whole arm	*SS18, ZNF521, MALT1, MADH4, FVT1, BCL2*
		20q13.13–20q13.33	50 442 828	62 317 398	11.87457	*GNAS, SS18L1*
		Xp22.13–Xp11.22	18 593 051	49 297 523	30.704472	*TFE3, SSX4, GATA1, SSX1 , WAS*
	15	3q12.1–3q29	99 594 845	197 114 668	97.519823	*MDS1, TFG, CBLB, ZNF9, GATA2, RPN1, FOXL2, GMPS, MLF1, EVI1, PIK3CA, BCL6, EIF4A2, ETV5, LPP, TFRC*
	22	10q22.2–10q26.3*	75 028 193	132 221 295	57.193102	*BMPR1A, MYST4, PTEN, NFKB2, TLX1, TNFRSF6, SUFU, FGFR2*
	24	1p	Whole arm	Whole arm	Whole arm	*RBM15, TRIM33, NRAS, NOTCH2, BCL10, SIL, EPS15, TAL1, SFPQ,THRAP3, MYCL1, MUTYH, LCK,MDS2, SDHB,PRDM16, PAX7, RPL22, MPL*
		1q	Whole arm	Whole arm	Whole arm	*PDE4DIP, BCL9, IRTA1, MUC1, AF1Q, ARNT, SDHC, PRCC, NTRK1, HRPT2, TPM3, FCGR2B, PBX1, PMX1, ABL2, TPR, ELK4, MDM4, SLC45A3, FH*
		10q22.2–10q26.3*	74 940 617	134 813 136	59.872519	*BMPR1A, MYST4, PTEN, NFKB2, TLX1, TNFRSF6, SUFU, FGFR2*
		14q22.3–14q32.33	53 559 881	102 230 659	48.670778	*KTN1, RAD51L1, GPHN*
	27	1p36.33–1p13.2	1 308 770	114 590 824	113.282054	*BCL10, SIL, EPS15, TAL1, SFPQ, THRAP3, MYCL1, MUTYH, LCK, MDS2, SDHB, PRDM16, PAX7, RPL22*
		9p24.3–9p13.3	264 108	35 051 504	34.787396	*CDKN2A- p14ARF, CDKN2A -p16(INK4a), MLLT3, PSIP2, JAK2*
	29	2p25.3–2p12	124 249	82 139 344	82.015095	*REL, IGK@ ,BCL11A, MSH6, EML4, MSH2, NCOA1, ALK, MYCN*
	31	1p35.2–1p31.2	30 984 284	59 013 240	28.028956	*SIL, EPS15, TAL1, SFPQ,THRAP3, MYCL1, MUTYH, LCK*
		1q23.2	156 672 464	157 185 184	0.51272	
		3p26.3–3p24.3	79 972	18 006 232	17.92626	*PPARG, RAF1, VHL, XPC, SRGAP3, FANCD2*
		3p24.3–3p24.1	20 755 592	29 221 196	8.465604	
		4p16.3–4p1533	344 051	14 519 067	14.175016	*WHSC1, FGFR3*
		4q22.3–4q31.21	94 588 552	143 180 768	48.592216	*TET2, IL2*
		4q31.23	149 715 072	149 730 992	0.01592	
250K		5q21.1	99 140 632	99 692 424	0.551792	
		5q23.1–5q32	117 033 848	146 035 968	29.00212	
		6p25.3–6p24.3	119 769	8 827 918	8.708149	*IRF4*

Table 1 Continued

SNP probes	*Sample#*	*Chromosome/ cytoband*	*Start*	*End*	*Minimal region (Mb)*	*Cancer-related genes*
		7q11.23–7q21.2	75 341 256	90 787 048	15.445792	
		8p23.2–8p21.1	198 834	6 508 840	6.310006	
		9q21.11–9q34.3	68 854 248	138 262 432	69.408184	*GNAQ, SYK, NR4A3, FANCC, PTCH, XPA, OMD, FNBP1, TAL2, CEP1, BRD3, SET, TSC1, NUP214, ABL1*
		10q25.3–10q26.3	117 468 544	135 293 424	17.82488	*FGFR2*
		13q21.2–13q34	60 518 320	114 054 472	53.536152	*ERCC5*
		17p13.1–17p12	83 173	14 791 705	14.708532	*RAB5EP, TP53, USP6, PER1*
		17q24.3–17q25.3	66 106 416	78 531 856	12.42544	*ASPSCR1, CANT1, ALO17*
		20p13–20p12.1	165 074	15 279 007	15.113933	
		21q21.2–21q21.3	25 499 006	26 046 936	0.54793	

Abbreviation: SNP, single-nucleotide polymorphism.
*Regions including the locus of PTEN.

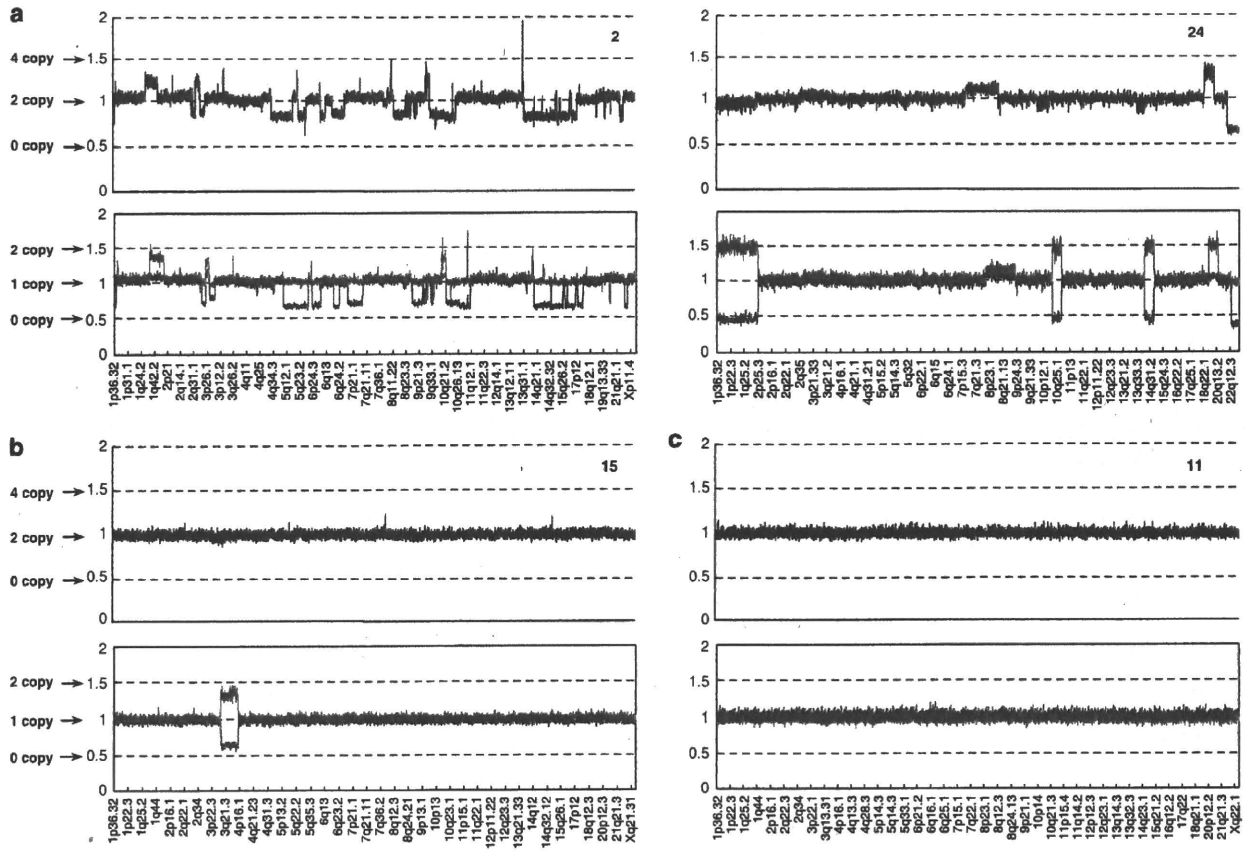

Figure 2 SNP array 'karyograms' (50K) of representative tumors. In each graph, the top shows the total copy number and the bottom shows the allele-specific copy number. CIN status is classified according to the number of loci with chromosomal imbalances. (**a**) Karyograms of two CIN-extensive tumors. CNN LOHs are predominantly detected in one sample at 1p, 1q, 10q22.2–26.3 and 14q22–32 (*right*). (**b**) Karyogram of one CIN-intermediate tumor. (**c**) Karyogram of one CIN-negative tumor.

ate. The SNP array 'karyograms' of representative tumors are shown in Figure 2. We classified tumors with five or more loci of copy alterations as CIN-extensive (Figure 2a), those with one to four loci as CIN-intermediate (Figure 2b), and those without any copy alterations as CIN-negative (Figure 2c). The karyograms of the remaining tumors are available in Supplementary Figure 1. In this classification, 9 out of 31 (29%) tumors were CIN-extensive, 17 (55%) were CIN-intermediate and 5 (16%) were CIN-negative (Figure 1). Whole arm chromosomal alterations were more frequently observed in CIN-extensive than in CIN-intermediate tumors (Figure 1 and Supplementary Figure 1).

Table 2 Status of microsatellite instability (MSI) and chromosomal instability (CIN)

	No.	*D2S123*	*D5S346*	*D17S250*	*BAT25*	*BAT26*	*CIN*
	24	+	+	+	+	+	Ext
	6	+	+	+	+	+	Int
	10	+	+	+	+	+	Int
	15	+	−	+	+	+	Int
MSI-high	17	+	+	+	+	+	Int
	18	+	+	+	+	+	Int
	21	+	+	−	+	−	Int
	11	−	+	+	+	+	Neg
	19	+	−	−	+	+	Neg
	20	+	−	+	+	+	Neg
	2	−	−	−	−	−	Ext
	5	−	−	−	−	−	Ext
	8	−	−	NA	−	−	Ext
	12	−	−	−	−	−	Ext
	14	−	−	−	−	−	Ext
	25	−	−	−	−	−	Ext
	1	−	−	−	−	−	Int
MSS	3	−	−	−	−	−	Int
	4	−	−	−	−	−	Int
	7	−	−	−	−	−	Int
	9	−	−	−	−	−	Int
	13	−	−	−	−	−	Int
	22	−	−	−	−	−	Int
	23	−	−	−	−	−	Int
	16	−	−	−	−	−	Neg

Abbreviations: Ext, extensive; Int, intermediate; MSS, microsatellite stable; NA, not available; Neg, negative.

MSI-high is commonly coexistent with CIN-negative and CIN-intermediate, but rarely with CIN-extensive

In this study, MSI-high was detected in 10 out of 25 (40%) endometrial carcinomas, and microsatellite stable (MSS) in 15 out of 25 (60%) (Table 2). MSI-low was not detected in this study. MSI-high was detected in 1 of 7 (14%) in CIN-extensive, 6 of 14 (43%) in CIN-intermediate and 3 of 4 (75%) in CIN-negative tumors, suggesting an inverse correlation between CIN and MSI. As a result, 24 of 25 (96%) endometrial carcinomas were positive for genomic instability (MSI and/or CIN).

We analyzed the clinicopathological characteristics of CIN-extensive. No significant difference in age, differentiation, vascular invasion, clinical stage and myometrial invasion was observed between CIN-extensive and the others (Supplementary Table 4). Presence of CNN LOH also does not have any significant associations in these factors (data not shown). MSI-high was correlated with vascular invasion ($P=0.049$), and shows a tendency toward unfavorable clinicopathological features, such as deep myometrial invasion and old age (Supplementary Table 5).

CIN-extensive is a poor prognostic factor in endometrial carcinomas

By Kaplan–Meier analysis, MSI-high showed a trend to be a favorable prognostic factor ($P=0.069$) (Supplementary Figure 2a). Next, we analyzed 50K SNP array in the other 11 endometrial carcinomas using tumor DNA, in addition to the 31 tumors. In 42 tumors, the ratio of CIN-extensive, -intermediate and -negative is 26% (11/42), 52% (22/42) and 21% (9/42), respectively. Kaplan–Meier analysis revealed that CIN-extensive was a significant marker of poor prognosis ($P=0.0034$ by log-rank test, Figure 3). A worse prognosis of CIN-extensive, compared with CIN-intermediate ($P=0.0033$, Supplementary Figure 2b), suggests that not only the existence but also the degree of CIN is important in endometrial tumorigenesis. Stage III–IV and histological grade (grade 2 or 3) were also poor prognostic factors by univariate analysis (Table 3). Subsequently, multivariate analysis was conducted using these three poor prognostic factors. Only CIN-extensive was found to be a significant and independent predictor for poor survival (Table 3).

Frequent CNN LOH with homozygous PTEN *mutations in endometrial carcinomas*

In SNP array analysis, we detected deletions of *PTEN* locus in 8 out of 31 (26%) tumors: one with HD, four with CNN LOH (marked with an asterisk in Table 1) and three with LOH without gain of the opposite allele. We also evaluated *PTEN* mutations and detected the mutations in 16 of 22 (73%) tumors. Taken together, we found three patterns of biallelic *PTEN* alterations in a total of eight tumors (36%): three tumors with CNN LOH and a mutation, four with two mutations and one with HD (Supplementary Table 6). Monoallelic *PTEN* alterations were observed in 11 tumors (50%): nine with a mutation, one with CNN LOH and one with LOH (Supplementary Table 6). Only three (14%) tumors showed no genomic alterations in *PTEN*. In our previous study, we did not observe any *PTEN* hypermethylation in 53 endometrial carcinomas (Shoji *et al.*, 2009).

MSS tumors frequently possess chromosomal imbalances in genes associated with the Ras-PI3K pathway

MSI is thought to correlate with mutator phenotype, and is reported to possess *PTEN* mutations more frequently than MSS in endometrial carcinomas. Indeed, all the MSI-high tumors possess *PTEN* mutations, whereas 6 of 12 MSS tumors (50%) possess *PTEN* mutations ($P=0.015$) (Supplementary Table 6). On the other hand, we found that six out of seven (87%) tumors with chromosomal imbalances of *PTEN* were MSS, suggesting that chromosomal imbalances have significant roles in disrupting PTEN function in MSS tumors.

Next, we analyzed genomic alterations of the other Ras-PI3K-related genes (*NF1*, *K-Ras* and *PIK3CA*). We found mutations of *K-Ras* and *PIK3CA* in 2 (9%) and 6 (27%) out of 22 tumors, respectively. In addition to one HD (4%) and two LOH (8%) at the *NF1* locus, we found gains at the loci of *PIK3CA* (3q26.3) in four (16%) tumors and *K-Ras* (12p12.1) in four (16%) tumors. CNN LOH at the loci of *PIK3CA* was observed in two (8%) tumors, including one with a *PIK3CA* mutation.

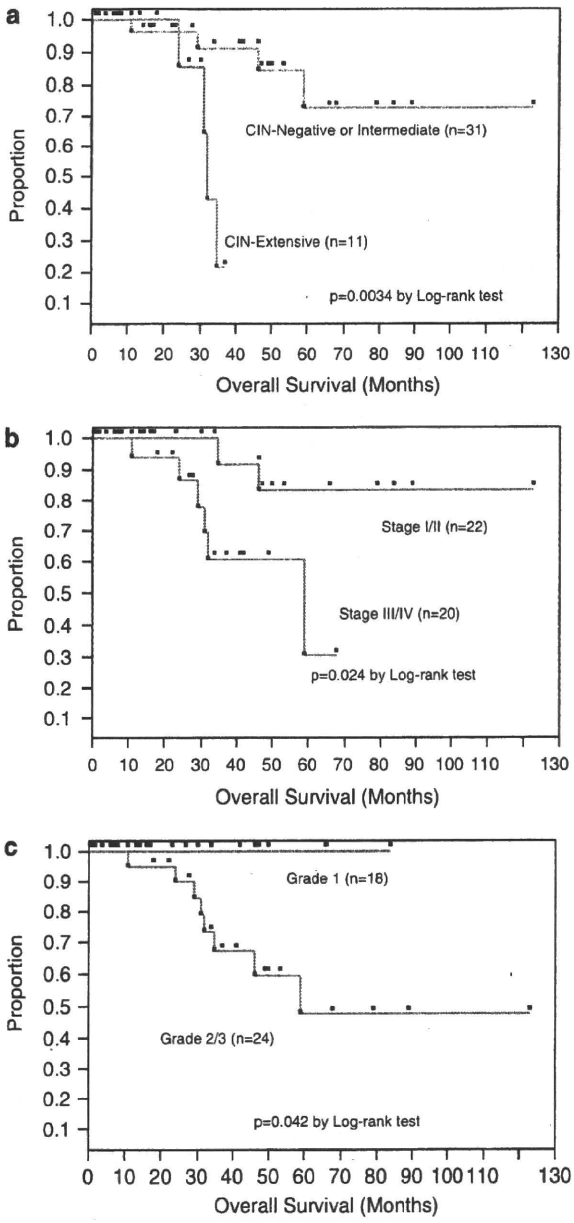

Figure 3 Overall survival of 42 endometrial carcinomas calculated according to the Kaplan–Meier method. (**a**) Survival of patients with CIN-extensive ($n=11$), compared with the others (CIN-negative or -intermediate ($n=31$). (**b**) Survival of stage III–IV patients ($n=20$) compared with stage I–II patients ($n=22$). (**c**) Survival of patients with histological grade 2–3 ($n=24$), compared with those with grade 1 ($n=18$).

We summarized the data of genomic alterations in the four genes (*PTEN*, *PIK3CA*, *K-Ras* and *NF1*) of the Ras-PI3K pathway (Table 4). In total, six out of the seven CIN-extensive tumors show deletion(s) in *PTEN* and/or *NF1*. Although the biological functions of copy number gains in *K-Ras* and *PIK3CA* are to be elucidated, all the seven CIN-extensive tumors show chromosomal imbalances in the loci of genes associated with the Ras-PI3K pathway, whereas 5 of the 14 CIN-intermediate tumors (36%) show such imbalances

Table 3 Univariate and multivariate analysis of prognostic factors for

Prognostic factor	P	
	Univariate	*Multivariate*
Age >60 (vs −60)	0.57	
Grade 2/3 (vs grade 1)	0.0099	0.070
FIGO stage III/IV (vs I/II)	0.026	0.27
Myometrial invasion >2/3 (vs <2/3)	0.62	
CIN-extensive (vs others)	0.011	0.048

Abbreviation: CIN, chromosomal instability.

($P=0.016$) (Table 4). In total, genetic mutations in the Ras-PI3K pathway and/or copy number losses in *PTEN* and/or *NF1* were detected in 20 of 22 tumors (91%). The 250K SNP array also revealed LOH in both *PTEN* and *NF1* genes in one of the six tumors.

Discussion

The relationship between CIN and MSI in endometrial carcinomas

Our analyses of genomic instability revealed that most of the endometrial carcinomas possess CIN and/or MSI. The positive ratios of CIN and MSI were 84% (21/25) and 40% (10/25), respectively. Inconsistent with colorectal cancer (Choi *et al.*, 2002), coexistence of MSI-high and positive CIN was observed in 28% (7/25) of our samples, especially in CIN-intermediate tumors (6/14=43%). This overlap might be explained, at least in part, by the detection of CNN LOH, as described below. The ratio of MSI-high (40%) in this study was higher than that (15–20%) in previous reports (Atkin, 2001; Woerner *et al.*, 2003), presumably because all the tumors in this study are endometrioid adenocarcinomas. In spite of correlation with lymphovascular invasion, MSI-high showed a trend of favorable prognosis. Positive MSI was also reported to correlate with advanced stage and deep myometrial invasion in endometrial carcinomas (Black *et al.*, 2006). On the other hand, we showed that CIN-extensive was an independent poor prognostic factor, without any significant associations with clinicopathological factors. These data suggest that the aggressive phenotype of CIN-extensive tumors is not predicted by any clinicopathological characteristics, and the favorable prognosis in MSI-high tumors might be explained by the inverse trend between MSI and CIN status. In this analysis, we added SNP array data from 11 specimens with only tumor DNA, in addition to 31 specimens with both tumor and normal DNA. We confirmed that the presence of CNN LOH affected the classification (CIN-extensive versus others) only in one of the 31 specimens with paired DNA. An additional 10 specimens classified by array CGH also supported the poor prognostic effect of CIN-extensive (data not shown). Therefore, our CIN classification would be also applicable to the data of either SNP array without normal DNA or array CGH. Although the SNP typing

Table 4 Mutations and copy number (CN) imbalances in Ras-PI3K pathway

CIN	*MSI*	*Number of genes with alterations*		*Types of alterations*					*Sample*
		Mutations	*CN imbalances*	*PTEN*	*Mutated codon(s)*	*PIK3CA*	*K-Ras*	*NF1*	
Negative									
1	High	2		Mut + Mut	(R173C/P213H)	Mut (D549N/T1025A)			19
2	High	1		Mut	(K164R)				11
3	High	1		Mut	(318-319: Del CTTA)				20
4	Negative	1		Mut	(L25F)				16
Intermediate									
1	High	3		Mut + Mut	(100; Ins A/291-293; Del 7bp)	Mut (H1047R)	Mut (G12C)		6
2	High	2	1	Mut + Mut	(164; Del A/268: Del A)	Mut (H1047R) + CNN LOH			15
3	High	2		Mut	(232; Ins A)	Mut (E542K)			10
4	High	2		Mut	(274; Del T)	Mut (H1047Y)			18
5	High	2		Mut	(137; Del A)		Mut (G13D)		21
6	High	1		Mut	(R173C)				17
7	Negative	2		Mut	(13; Ins C)	Mut (N1044K)			13
8	Negative	1		Mut + Mut	(R130G/R233*(stop))				4
9	Negative	1	2	Mut + CNN LOH	(291; Ins A)	CNN LOH			9
10	Negative	1	1	Mut	(L146*(stop))		Gain		23
11	Negative		1	CNN LOH					22
12	Negative								3
13	Negative	NA	1	NA		Gain			1
14	Negative	NA		NA					7
Extensive									
1	High	1	1	Mut + CNN LOH	(G132R)				24
2	Negative	1	1	Mut + CNN LOH	(R130G)				5
3	Negative		3	HD		Gain		HD	2
4	Negative		3	LOH		Gain	Gain	LOH	8
5	Negative		2			Gain		LOH	12
6	Negative		1				Gain		25
7	Negative	NA	2	LOH			Gain		14

Abbreviations: HD, homozygous deletion; PI3K, phosphatidylinositol 3′-kinase.

array or array CGH may not be currently cost-effective, defining CIN status will become more feasible with the prevalence of genome-wide analysis of each cancer. The information that all the patients with risk factors (such as lymph node metastasis and deep myometrial invasion) received adjuvant radiation and/or chemotherapy suggests that CIN-extensive might be also associated with sensitivity to adjuvant chemotherapy and/or radiotherapy. The loci of copy alterations in CIN-extensive did not frequently overlap with each other in our analyses (Figure 1). Rather, the region of copy alterations spreads to the entire genome. The numerous patterns of copy alterations in CIN-extensive tumors indicate that the degree of CIN itself, not the alterations of specific genes, might be a significant marker for tumor aggressiveness.

CNN LOH and HD in endometrial carcinomas

Recently, CNN LOH has been reported in various types of tumors at the loci of important genes that drive the carcinogenic process (Bacolod *et al.*, 2009; Tuna *et al.*, 2009). The ratio of CNN LOH was reported at 20–50% in several tumors, including leukemia, liver cancer and ovarian cancer (Raghavan *et al.*, 2005; Midorikawa *et al.*, 2006; Dunbar *et al.*, 2008; Walsh *et al.*, 2008). Considering the fact that only 28% of tumors were CIN-extensive, it is noteworthy that CNN LOH was positive in 42% of endometrial carcinomas. Especially, 3 of 14 CIN-intermediate tumors show CNN LOH alone without any other chromosomal gains and losses that would be overlooked by CGH. These results suggest that CNN LOH shares a significant ratio and may have key roles in endometrial carcinogenesis. We found one HD and one CNN LOH at the *CDKN2A* locus (9p21.3) and two CNN LOH at the *TP53* locus (17p13.1). These alterations have been reported in other types of malignancy such as of the colon, breast and leukocyte (Melcher *et al.*, 2007; Kawamata *et al.*, 2008; Walsh *et al.*, 2008). In gynecologic malignancies, HD at 9p21.3, 10q23.3, 17q11.2 and CNN LOH at 1p36.13–1p36.11, 13q31.1, 13q32.3–13q34, 17p13.2–17p11.2, 17q21.33–17q23.2, Xp21.1 and Xp11.4–Xp11.3 were also reported in ovarian cancer (Gorringe *et al.*, 2009). Thus, CNN

LOH and HD of specific tumor suppressor genes might be widespread in various types of tumors.

Copy number polymorphisms are known to be common in the human genome (Conrad *et al.*, 2006). Normalization of tumor samples to their matching normal germline DNA is a useful method to mask such copy number polymorphisms; however, copy number polymorphisms and interchromosomal segmental duplications can still masquerade as somatic alterations in tumors with extensive copy number imbalances (Gorringe and Campbell, 2008). In our analysis, one HD at 6q21.2 was suggested to be one of the germline CNVs. Thus, it is very important to exclude the possibility of germline CNVs in each HD region.

Biallelic PTEN inactivation and MSI status

The most frequent CNN LOH was 10q22.2–10q26.3, which includes *PTEN*. The ratio of LOH in *PTEN* has been reported to be 20–40% by microsatellite markers and approximately 15% by CGH (Sirchia *et al.*, 2000; Suehiro *et al.*, 2000; Toda *et al.*, 2001; Micci *et al.*, 2004; Levan *et al.*, 2006). In our analysis, four of seven LOH detected at the *PTEN* locus turned out to be CNN LOH, indicating that LOH of *PTEN* has been underestimated by CGH in endometrial carcinomas. Three of the four tumors with CNN LOH at *PTEN* possess homozygous *PTEN* mutations. In addition, HD of *PTEN* at 10q23 was also detected in one tumor. We previously reported multiple *PTEN* mutations in 9 out of 37 *PTEN* mutant tumors (Minaguchi *et al.*, 2001). Taken together, inactivation of *PTEN* is caused by various reasons, such as (1) a mutation and LOH without gain of the opposite allele, (2) homozygous mutations and CNN LOH, (3) HD and (4) mutations in both alleles. There might be other unknown mechanisms of biallelic *PTEN* inactivation, as 11 tumors showed monoallelic *PTEN* alterations in this study, including one tumor with CNN LOH at *PTEN*. *PTEN* mutations in endometrial carcinomas were reported to be more common in MSI-positive tumors, compared with MSS tumors (Bilbao *et al.*, 2006). In this study, all the three tumors with multiple *PTEN* mutations were MSI-high, whereas six out of seven tumors with *PTEN* deletion(s) were MSS. These data suggest that the mechanism of *PTEN* inactivation is affected by MSI status.

Prevalent genomic alterations in the Ras signaling pathway

The frequency of mutations in *K-Ras*, *PTEN* and *PIK3CA* in the Ras-PI3K pathway is remarkable in endometrial carcinomas. *NF1*, located at 17q11.2, functions as a negative regulator of the Ras signaling pathway (McCormick, 1995). Recently, CNN LOH surrounding the *NF1* locus was observed in juvenile myelomonocytic leukemia (Flotho *et al.*, 2007). Although inactivation of *NF1* has not been reported in endometrial carcinomas, we have detected one HD at 17q11.2 and three LOH at this locus in 31 samples (13%). Copy number losses in *NF1* suggest that there might be other types of alterations in this gene in endometrial carcinomas, such as inactivating mutations reported in glioblastomas (Cancer Genome Atlas Research Network, 2008).

Amplifications of *PIK3CA* (3q26.3) and *K-Ras* (12p12.1) loci are other possible mechanisms of alterations. SNP array analysis revealed copy number gains at the locus of *K-Ras* (13%) and *PIK3CA* (13%), supporting the previous reports (Oda *et al.*, 2005; Salvesen *et al.*, 2009). One of the two tumors with CNN LOH at the *PIK3CA* locus contains a 'hot spot' *PIK3CA* mutation (H1047R), which might result in increased activity of mutant p110alpha. However, it is to be elucidated whether gains (and CNN LOH without a mutation in the opposite allele) at the loci of *PIK3CA* and *K-Ras* are in fact targeting these genes. Comprehensive analyses of genomic alterations in the Ras-PI3K pathway revealed that genomic alterations in the Ras-PI3K pathway are extensively common, as observed in Table 4. These results suggest that the activation of this pathway might be a critical step in endometrial tumorigenesis and that targeting this pathway might be a promising therapeutic strategy in endometrial carcinomas.

Materials and methods

Tumor samples and genomic DNA

Surgical samples were obtained from a total of 42 patients with primary endometrial carcinomas (endometrioid adenocarcinomas) who underwent resection of their tumors at the University of Tokyo Hospital. All the 42 patients were treated as previously described (Onda *et al.*, 1997). Briefly, they received primary surgery, including hysterectomy, bilateral salpingo-oophorectomy and systematic lymphadenectomy. Whole-pelvis irradiation was indicated for stage I–III patients with at least one of the following factors: deep myometrial invasion, positive lymph nodes, adnexal metastases and pelvic peritoneal metastases. The stage III patients with either adnexal/peritoneal involvement or aortic node metastases were treated with three cycles of platinum-based chemotherapy before radiation therapy. Stage IV patients were treated postoperatively with five cycles of platinum-based chemotherapy. All the recurrent patients received platinum-based chemotherapy.

All of the patients provided informed consent for the research use of their samples and the collection, and the use of tissues for this study was approved by the appropriate institutional ethics committees. The fresh-frozen tumors were embedded in OCT compound, and the 4-μm tissue sections were stained with hematoxylin and eosin. We confirmed that each section contains a high purity of tumor epithelium (>60%) and used those sections for DNA extraction. Genomic DNA was isolated from the tumor sections or lymphocyte pellets using a QIAamp DNA Mini Kit (Qiagen, Valencia, CA, USA), according to the manufacturer's specifications. Paired genomic DNA was also extracted as a control through blood samples in 31 out of 42 patients. The clinical status of these 42 patients was summarized in Supplementary Table 1.

SNP array

SNP array was performed in 31 clinical samples with paired tumor DNA and normal DNA, and 11 clinical samples with tumor DNA alone. Experimental procedures for GeneChip

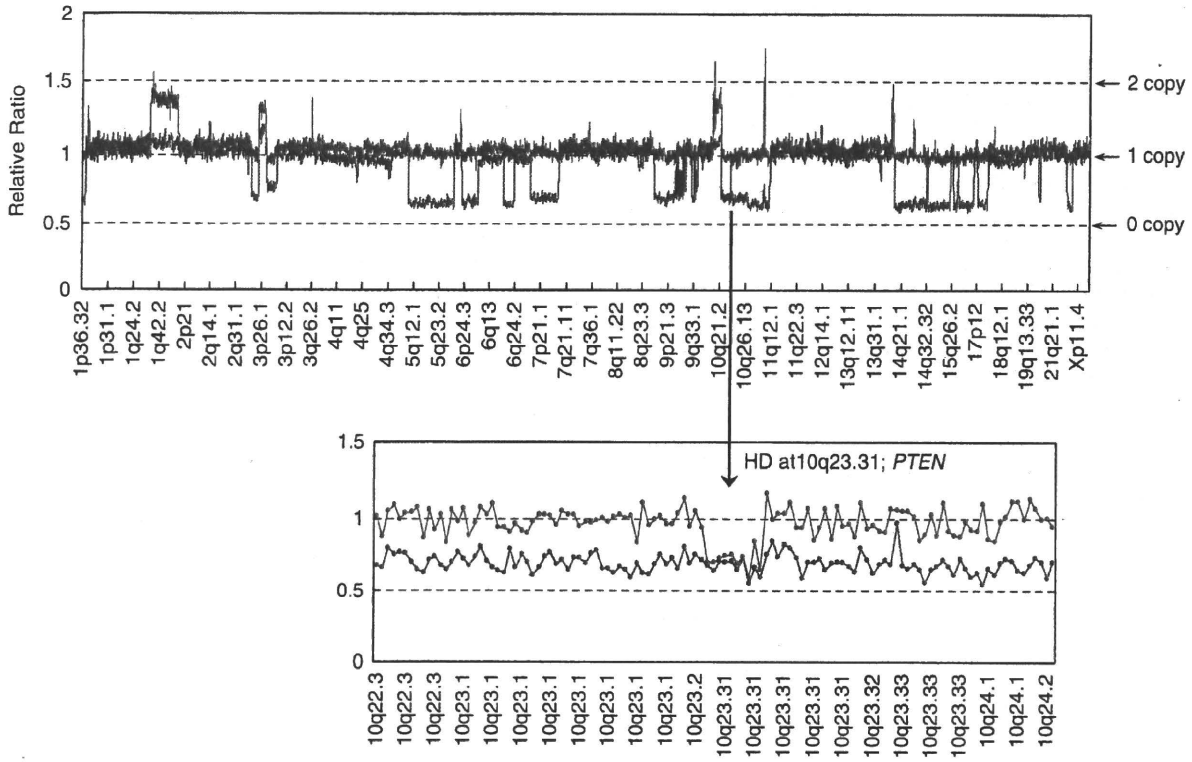

Figure 4 Detection of allele-specific copy number alterations, including homozygous deletions (HD), using a human mapping 50K SNP array technology. Red bar corresponds to the allele with a higher copy number, and blue bar to that with a lower copy number. This representative sample shows LOH at multiple loci (top). Inside the LOH, chromosome 10q23.3 is homozygously deleted as shown in the bottom.

were performed according to GeneChip Expression Analysis Technical Manual (Affymetrix, Santa Clara, CA, USA), using a Human mapping 50K Xba I Array in 36 out of 42 samples. The remaining six samples with paired DNA were analyzed with a Human mapping 250K Nsp Array (Affymetrix).

Genome imbalance map

The GIM algorithm was applied to the raw data of endometrial cancer and peripheral blood obtained from SNP arrays. We previously reported that the purity of tumor epithelium at 50% is sufficient for the GIM algorithm (Ishikawa *et al*., 2005). The basic concept of GIM involves the normalization of probe level signals, as previously described (Ishikawa *et al*., 2005). Briefly, the signal intensity ratio between the raw signal intensity from the cancer and paired normal samples was calculated from the perfect match probes for each SNP locus by taking the median after omitting the highest and lowest values. Second, we calculated the adjusted ratio, which is the raw ratio divided by the expected ratio. The expected ratio is calculated by adjusting several parameters for each experiment, for example, length of *Xba* I (or Nsp) fragment, percentage of GC of *Xba* I (or Nsp) fragments, local GC content, hybridization-free energy of 25-mer probe sequences and genomic mean of signal intensity of perfect match probes from reference sample. For allele-specific copy number analysis in this GIM algorism, the relative ratio of 0.5, 1 and 1.5 theoretically corresponds to 0, 1 and 2 copies, respectively (Figure 4). We detected allele-specific copy number alterations, using the cutoff relative ratio of >1.3 (1.6 copies) for gain and <0.7 (0.4 copies) for loss in each region. Total copy number alterations were also detected by using the cutoff relative ratio of >1.15 (2.6 copies) for gain and <0.85 (1.4 copies) for loss.

MSI analysis

Genomic DNAs extracted from the samples were used to study MSI status using five fluorescence-labeled microsatellite markers (BAT25, BAT26, D2S123, D5S346 and D17S250). Primer sequences have been previously described (Loukola *et al*., 2001). PCR reactions were performed with KOD plus DNA Polymerase (TOYOBO, Osaka, Japan). The PCR conditions were as follows: 94°C for 2 min; 30 cycles of 94°C for 15 s, 54–60°C for 30 s, 68°C for 30 s, followed by a final extension at 68°C for 2 min. After PCR, 1 μl of the product (×30 diluted) was mixed with 10 μl Hi-di Formamide and a size marker. This product was denatured at 95°C for 5 min and cooled on ice before loading onto ABI 3130 Genetic Analyzer (Applied Biosystems, Foster City, CA, USA). Results were analyzed by Genemapper Software Version 4.0 (Applied Biosystems). Determination of MSI status was made according to the presence of mutant alleles in tumor DNA compared with blood DNA. MSI status was determined as follows: tumors with two or more positive MSI markers as MSI-H, one positive MSI marker as MSI-L, and no positive MSI markers as MSS (microsatellite stable).

Mutational analysis

Mutations for *PTEN* (exon1-8), *K-Ras* (exon1 and 2) and *PIK3CA* (exon9 and 20) were analyzed as previously described (Minaguchi *et al*., 2001; Oda *et al*., 2005, 2008).

Statistical analysis

The association of variables related to clinical characteristics was evaluated by Fisher's exact test. The *P*-values obtained in all tests were considered to be significant at $P<0.05$. Survival

curves were constructed using the Kaplan–Meier method and compared with the log-rank test. The analyses were carried out using the JMP 7 statistics package (SAS Institute, Cary, NC, USA). Multivariate analysis was evaluated by Cox's proportional hazards model.

Conclusion

We comprehensively analyzed genomic alterations in endometrial carcinomas. The novel classification by the number of chromosomal imbalances revealed that CIN-extensive is an independent poor prognostic factor. As the status of genomic instability is not morphologically recognized, our CIN classification would provide a useful biomarker for prognosis in endometrial carcinomas. SNP array analysis revealed CNN LOH at 42% and HD at 10%, including the locus of *PTEN*. Our data indicated that alterations in the Ras-PI3K pathway are extensively prevalent in endometrial carcinomas through both chromosomal imbalances and genetic mutations.

Conflict of interest

The authors declare no conflict of interest.

Acknowledgements

We thank Hiroko Meguro, Akira Watanabe, Jennifer Okada, Toshiharu Yasugi, Kei Kawana, Takahide Arimoto, Akira Tsuchiya, Osamu Hiraike-Wada, Kenbun Sone, Yuichiro Miyamoto, Haruko Hiraike, Katsuyuki Adachi, Shiho Miura and Ayako Tomio for support and assistance. This work was supported by the Ministry of Education, Science, Sports and Culture Grant Number: Scientific Research (S) 16101006, Scientific Research on Priority Areas 17015008, Ministry of Education, Culture, Sports, Science and Technology of Japan on Priority Area; Grant Number: 20014007, and Core Research for Evolutional Science and Technology (CREST), Japan Science and Technology Agency (JST) (to H Aburatani); by the Grant-in-Aid for Scientific Research (C), Grant Number 19599005 and the Grant-in-Aid for Young Scientists (B), Grant Number 21791544 from the Ministry of Education, Culture, Sports, Science and Technology of Japan (to K Oda); by the Grant-in-Aid for Scientific Research on Priority Areas 'Applied Genomics', Grant Number 20018005, from the Ministry of Education, Culture, Sports, Science and Technology of Japan and Industrial Technology Research Grant Program from New Energy and Industrial Technology Development Organization (NEDO) of Japan (to S Ishikawa).

References

An HJ, Logani S, Isacson C, Ellenson LH. (2004). Molecular characterization of uterine clear cell carcinoma. *Mod Pathol* **17**: 530–537.

Arabi H, Guan H, Kumar S, Cote M, Bandyopadhyay S, Shah J *et al.* (2009). Impact of microsatellite instability (MSI) on survival in high grade endometrial carcinoma. *Gynecol Oncol* **113**: 153–158.

Atkin NB. (2001). Microsatellite instability. *Cytogenet Cell Genet* **92**: 177–181.

Bacolod MD, Schemmann GS, Giardina SF, Paty P, Notterman DA, Barany F. (2009). Emerging paradigms in cancer genetics: some important findings from high-density single nucleotide polymorphism array studies. *Cancer Res* **69**: 723–727.

Bilbao C, Rodríguez G, Ramírez R, Falcón O, León L, Chirino R *et al.* (2006). The relationship between microsatellite instability and PTEN gene mutations in endometrial cancer. *Int J Cancer* **119**: 563–570.

Black D, Soslow RA, Levine DA, Tornos C, Chen SC, Hummer AJ *et al.* (2006). Clinicopathologic significance of defective DNA mismatch repair in endometrial carcinoma. *J Clin Oncol* **24**: 1745–1753.

Cancer Genome Atlas Research Network (2008). Comprehensive genomic characterization defines human glioblastoma genes and core pathways. *Nature* **455**: 1061–1068.

Carpten JD, Faber AL, Horn C, Donoho GP, Briggs SL, Robbins CM *et al.* (2007). A transforming mutation in the pleckstrin homology domain of AKT1 in cancer. *Nature* **448**: 439–444.

Cheng JQ, Godwin AK, Bellacosa A, Taguchi T, Franke TF, Hamilton TC *et al.* (1992). AKT2, a putative oncogene encoding a member of a subfamily of protein-serine/threonine kinases, is amplified in human ovarian carcinomas. *Proc Natl Acad Sci USA* **89**: 9267–9271.

Choi SW, Lee KJ, Bae YA, Min KO, Kwon MS, Kim KM *et al.* (2002). Genetic classification of colorectal cancer based on chromosomal loss and microsatellite instability predicts survival. *Clin Cancer Res* **8**: 2311–2322.

Conrad DF, Andrews TD, Carter NP, Hurles ME, Pritchard JK. (2006). A high-resolution survey of deletion polymorphism in the human genome. *Nat Genet* **38**: 75–81.

Doll A, Abal M, Rigau M, Monge M, Gonzalez M, Demajo S *et al.* (2008). Novel molecular profiles of endometrial cancer-new light through old windows. *J Steroid Biochem Mol Biol* **108**: 221–229.

Dunbar AJ, Gondek LP, O'Keefe CL, Makishima H, Rataul MS, Szpurka H *et al.* (2008). 250K single nucleotide polymorphism array karyotyping identifies acquired uniparental disomy and homozygous mutations, including novel missense substitutions of c-Cbl, in myeloid malignancies. *Cancer Res* **68**: 10349–10357.

Enomoto T, Inoue M, Perantoni AO, Buzard GS, Miki H, Tanizawa O *et al.* (1991). K-ras activation in premalignant and malignant epithelial lesions of the human uterus. *Cancer Res* **51**: 5308–5314.

Fitzgibbon J, Smith LL, Raghavan M, Smith ML, Debernardi S, Skoulakis S *et al.* (2005). Association between acquired uniparental disomy and homozygous gene mutation in acute myeloid leukemias. *Cancer Res* **65**: 9152–9154.

Flotho C, Steinemann D, Mullighan CG, Neale G, Mayer K, Kratz CP *et al.* (2007). Genome-wide single-nucleotide polymorphism analysis in juvenile myelomonocytic leukemia identifies uniparental disomy surrounding the NF1 locus in cases associated with neurofibromatosis but not in cases with mutant RAS or PTPN11. *Oncogene* **26**: 5816–5821.

Geigl JB, Obenauf AC, Schwarzbraun T, Speicher MR. (2008). Defining 'chromosomal instability'. *Trends Genet* **24**: 64–69.

Gorringe KL, Campbell IG. (2008). High-resolution copy number arrays in cancer and the problem of normal genome copy number variation. *Genes Chromosomes Cancer* **47**: 933–938.

Gorringe KL, Jacobs S, Thompson ER, Sridhar A, Qiu W, Choong DY *et al.* (2007). High-resolution single nucleotide polymorphism array analysis of epithelial ovarian cancer reveals numerous microdeletions and amplifications. *Clin Cancer Res* **13**: 4731–4739.

Gorringe KL, Ramakrishna M, Williams LH, Sridhar A, Boyle SE, Bearfoot JL *et al.* (2009). Are there any more ovarian tumor suppressor genes? A new perspective using ultra high-resolution copy number and loss of heterozygosity analysis. *Genes Chromosomes Cancer* **48**: 931–942.

Grady WM. (2004). Genomic instability and colon cancer. *Cancer Metastasis Rev* **23**: 11–27.

Hirasawa A, Aoki D, Inoue J, Imoto I, Susumu N, Sugano K *et al.* (2003). Unfavorable prognostic factors associated with high frequency of microsatellite instability and comparative genomic hybridization analysis in endometrial cancer. *Clin Cancer Res* **9**: 5675–5682.

Ishikawa S, Komura D, Tsuji S, Nishimura K, Yamamoto S, Panda B *et al.* (2005). Allelic dosage analysis with genotyping microarrays. *Biochem Biophys Res Commun* **333**: 1309–1314.

Kawamata N, Ogawa S, Zimmermann M, Kato M, Sanada M, Hemminki K *et al.* (2008). Molecular allelokaryotyping of pediatric acute lymphoblastic leukemias by high-resolution single nucleotide polymorphism oligonucleotide genomic microarray. *Blood* **111**: 776–784.

Komura D, Shen F, Ishikawa S, Fitch KR, Chen W, Zhang J *et al.* (2006). Genome-wide detection of human copy number variations using high-density DNA oligonucleotide arrays. *Genome Res* **16**: 1575–1584.

Kong D, Suzuki A, Zou TT, Sakurada A, Kemp LW, Wakatsuki S *et al.* (1997). PTEN1 is frequently mutated in primary endometrial carcinomas. *Nat Genet* **17**: 143–144.

Kong D, Yamori T. (2008). Phosphatidylinositol 3-kinase inhibitors: promising drug candidates for cancer therapy. *Cancer Sci* **99**: 1734–1740.

Kralovics R, Passamonti F, Buser AS, Teo SS, Tiedt R, Passweg JR *et al.* (2005). A gain-of-function mutation of JAK2 in myeloproliferative disorders. *N Engl J Med* **352**: 1779–1790.

Kratz CP, Steinemann D, Niemeyer CM, Schlegelberger B, Koscielniak E, Kontny U *et al.* (2007). Uniparental disomy at chromosome 11p15.5 followed by HRAS mutations in embryonal rhabdomyosarcoma: lessons from Costello syndrome. *Hum Mol Genet* **16**: 374–379.

Levan K, Partheen K, Osterberg L, Helou K, Horvath G. (2006). Chromosomal alterations in 98 endometrioid adenocarcinomas analyzed with comparative genomic hybridization. *Cytogenet Genome Res* **115**: 16–22.

Li J, Yen C, Liaw D, Podsypanina K, Bose S, Wang SI *et al.* (1997). PTEN, a putative protein tyrosine phosphatase gene mutated in human brain, breast, and prostate cancer. *Science* **275**: 1943–1947.

Loukola A, Eklin K, Laiho P, Salovaara R, Kristo P, Jarvinen H *et al.* (2001). Microsatellite marker analysis in screening for hereditary nonpolyposis colorectal cancer (HNPCC). *Cancer Res* **61**: 4545–4549.

Lynch TJ, Bell DW, Sordella R, Gurubhagavatula S, Okimoto RA, Brannigan BW *et al.* (2004). Activating mutations in the epidermal growth factor receptor underlying responsiveness of non-small-cell lung cancer to gefitinib. *N Engl J Med* **350**: 2129–2139.

Maira SM, Stauffer F, Schnell C, Garcia Echeverria C. (2009). PI3K inhibitors for cancer treatment: where do we stand? *Biochem Soc Trans* **37**: 265–272.

McCormick F. (1995). Ras signaling and NF1. *Curr Opin Genet Dev* **5**: 51–55.

Melcher R, Al Taie O, Kudlich T, Hartmann E, Maisch S, Steinlein C *et al.* (2007). SNP-Array genotyping and spectral karyotyping reveal uniparental disomy as early mutational event in MSS- and MSI-colorectal cancer cell lines. *Cytogenet Genome Res* **118**: 214–221.

Micci F, Teixeira MR, Haugom L, Kristensen G, Abeler VM, Heim S. (2004). Genomic aberrations in carcinomas of the uterine corpus. *Genes Chromosomes Cancer* **40**: 229–246.

Midorikawa Y, Yamamoto S, Ishikawa S, Kamimura N, Igarashi H, Sugimura H *et al.* (2006). Molecular karyotyping of human hepatocellular carcinoma using single-nucleotide polymorphism arrays. *Oncogene* **25**: 5581–5590.

Minaguchi T, Yoshikawa H, Oda K, Ishino T, Yasugi T, Onda T *et al.* (2001). PTEN mutation located only outside exons 5, 6, and 7 is an independent predictor of favorable survival in endometrial carcinomas. *Clin Cancer Res* **7**: 2636–2642.

Oda K, Okada J, Timmerman L, Rodriguez Viciana P, Stokoe D, Shoji K *et al.* (2008). PIK3CA cooperates with other phosphatidylinositol 3′-kinase pathway mutations to effect oncogenic transformation. *Cancer Res* **68**: 8127–8136.

Oda K, Stokoe D, Taketani Y, McCormick F. (2005). High frequency of coexistent mutations of PIK3CA and PTEN genes in endometrial carcinoma. *Cancer Res* **65**: 10669–10673.

Onda T, Yoshikawa H, Mizutani K, Mishima M, Yokota H, Nagano H *et al.* (1997). Treatment of node-positive endometrial cancer with complete node dissection, chemotherapy and radiation therapy. *Br J Cancer* **75**: 1836–1841.

Parkin DM. (2001). Global cancer statistics in the year 2000. *Lancet Oncol* **2**: 533–543.

Raghavan M, Lillington DM, Skoulakis S, Debernardi S, Chaplin T, Foot NJ *et al.* (2005). Genome-wide single nucleotide polymorphism analysis reveals frequent partial uniparental disomy due to somatic recombination in acute myeloid leukemias. *Cancer Res* **65**: 375–378.

Rowan A, Halford S, Gaasenbeek M, Kemp Z, Sieber O, Volikos E *et al.* (2005). Refining molecular analysis in the pathways of colorectal carcinogenesis. *Clin Gastroenterol Hepatol* **3**: 1115–1123.

Ryan AJ, Susil B, Jobling TW, Ochler MK. (2005). Endometrial cancer. *Cell Tissue Res* **322**: 53–61.

Salvesen HB, Carter SL, Mannelqvist M, Dutt A, Getz G, Stefansson IM *et al.* (2009). Integrated genomic profiling of endometrial carcinoma associates aggressive tumors with indicators of PI3 kinase activation. *Proc Natl Acad Sci USA* **106**: 4834–4839.

Samuels Y, Wang Z, Bardelli A, Silliman N, Ptak J, Szabo S *et al.* (2004). High frequency of mutations of the PIK3CA gene in human cancers. *Science* **304**: 554.

Shayesteh L, Lu Y, Kuo WL, Baldocchi R, Godfrey T, Collins C *et al.* (1999). PIK3CA is implicated as an oncogene in ovarian cancer. *Nat Genet* **21**: 99–102.

Shoji K, Oda K, Nakagawa S, Hosokawa S, Nagae G, Uehara Y *et al.* (2009). The oncogenic mutation in the pleckstrin homology domain of AKT1 in endometrial carcinomas. *Br J Cancer* **101**: 145–148.

Sirchia SM, Sironi E, Grati FR, Serafini P, Garagiola I, Rossella F *et al.* (2000). Losses of heterozygosity in endometrial adenocarcinomas: positive correlations with histopathological parameters. *Cancer Genet Cytogenet* **121**: 156–162.

Slamon DJ, Godolphin W, Jones LA, Holt JA, Wong SG, Keith DE *et al.* (1989). Studies of the HER-2/neu proto-oncogene in human breast and ovarian cancer. *Science* **244**: 707–712.

Stokoe D, Stephens LR, Copeland T, Gaffney PR, Reese CB, Painter GF *et al.* (1997). Dual role of phosphatidylinositol-3,4,5-trisphosphate in the activation of protein kinase B. *Science* **277**: 567–570.

Suehiro Y, Umayahara K, Ogata H, Numa F, Yamashita Y, Oga A *et al.* (2000). Genetic aberrations detected by comparative genomic hybridization predict outcome in patients with endometrioid carcinoma. *Genes Chromosomes Cancer* **29**: 75–82.

Tashiro H, Lax SF, Gaudin PB, Isacson C, Cho KR, Hedrick L. (1997). Microsatellite instability is uncommon in uterine serous carcinoma. *Am J Pathol* **150**: 75–79.

Teh MT, Blaydon D, Chaplin T, Foot NJ, Skoulakis S, Raghavan M *et al.* (2005). Genomewide single nucleotide polymorphism microarray mapping in basal cell carcinomas unveils uniparental disomy as a key somatic event. *Cancer Res* **65**: 8597–8603.

Toda T, Oku H, Khaskhely NM, Moromizato H, Ono I, Murata T. (2001). Analysis of microsatellite instability and loss of heterozygosity in uterine endometrial adenocarcinoma. *Cancer Genet Cytogenet* **126**: 120–127.

Tuna M, Knuutila S, Mills GB. (2009). Uniparental disomy in cancer. *Trends Mol Med* **15**: 120–128.

Vogelstein B, Fearon ER, Hamilton SR, Kern SE, Preisinger AC, Leppert M *et al.* (1988). Genetic alterations during colorectal-tumor development. *N Engl J Med* **319**: 525–532.

Walsh CS, Ogawa S, Scoles DR, Miller CW, Kawamata N, Narod SA *et al.* (2008). Genome-wide loss of heterozygosity and uniparental disomy in BRCA1/2-associated ovarian carcinomas. *Clin Cancer Res* **14**: 7645–7651.

Weber JC, Meyer N, Pencreach E, Schneider A, Guerin E, Neuville A *et al.* (2007). Allelotyping analyses of synchronous primary and metastasis CIN colon cancers identified different subtypes. *Int J Cancer* **120**: 524–532.

Woerner SM, Benner A, Sutter C, Schiller M, Yuan YP, Keller G *et al.* (2003). Pathogenesis of DNA repair-deficient cancers: a statistical meta-analysis of putative Real Common Target genes. *Oncogene* **22**: 2226–2235.

Supplementary Information accompanies the paper on the Oncogene website (http://www.nature.com/onc)

Cancer Science
The official journal of the Japanese Cancer Association

Potent *in vitro* and *in vivo* antitumor effects of MDM2 inhibitor nutlin-3 in gastric cancer cells

Shinji Endo,[1] Kenji Yamato,[2] Sachiko Hirai,[1] Toshikazu Moriwaki,[1] Kuniaki Fukuda,[1] Hideo Suzuki,[1] Masato Abei,[1] Ichiro Nakagawa[2] and Ichinosuke Hyodo[1,3]

[1]Department of Gastroenterology and Hepatology, Institute of Clinical Medicine, Graduate School of Comprehensive Human Sciences, University of Tsukuba, Tsukuba; [2]Section of Bacterial Pathogenesis, Graduate School of Medical and Dental Science, Tokyo Medical and Dental University, Tokyo, Japan

(Received August 30, 2010/Revised November 29, 2010/Accepted December 1, 2010/Accepted manuscript online December 7, 2010)

The tumor suppressor gene *p53* is the most frequently mutated gene in human cancers. However, its mutation rate is relatively low in gastric cancer compared with other cancers. In this study, we investigated the mechanisms underlying the antitumor effects of nutlin-3, an inhibitor of human homolog of murine double minute 2 (MDM2). MDM2 is a negative regulator of p53. Four gastric cancer cell lines with wild-type *p53* (wt *p53*) and three with mutant-type *p53* (mt *p53*) were analyzed for MDM2 and MDM4 expression by immunoblotting, and for their gene amplification by quantitative real-time PCR. Moreover, the viability of cells exposed to nutlin-3 was examined by WST-8 assay, and the expression of p53 and its downstream genes was analyzed by immunoblotting. Nutlin-3 stabilized p53 and increased the expression of $p21^{WAF1}$ and Noxa, and cleaved poly (ADP)-ribose polymerase regardless of the pre-expression levels of MDM2 and MDM4 in gastric cancer cells with wt *p53*. Flow cytometry revealed that nutlin-3 arrested the cell cycle in G_1 phase and induced apoptosis in the cell lines. These nutlin-3 effects were not observed in the cell lines with mt *p53*. Nutlin-3 exerted additive or synergistic cytotoxicity in combination with 5-fluorouracil or cisplatin in most cell lines with wt *p53*. An *in vivo* antitumor effect of nutlin-3 alone and its additive augmentation by 5-fluorouracil were confirmed in an MDM2 overexpressed xenograft tumor model. Nutlin-3 showed potent antitumor activity against human gastric cancer cells with wt *p53* and shows promise as a single agent and in combination with conventional anticancer drugs. (*Cancer Sci*, doi: 10.1111/j.1349-7006.2010.01821.x, 2011)

The tumor suppressor gene *p53* plays a central role in the regulation of the cell cycle, DNA repair, apoptosis, and senescence.[1–3] Deleted or mutated p53 occurs in approximately half of human cancers, indicating that a substantial proportion of human carcinogenesis is caused by dysfunction of the p53 pathway.[4] In human gastric cancer, the rate of *p53* mutation is approximately 30%.[5,6] To date, the efficacy of p53 pathway activation in controlling gastric cancer with wild-type *p53* (wt *p53*) has not yet been fully elucidated.

Human homolog of murine double minute 2 (MDM2) negatively regulates p53.[7] MDM2 is a p53-specific E3 ubiquitin ligase that mediates the ubiquitin-dependent degradation of p53.[8,9] Moreover, MDM2 can bind to the p53 transactivation domain and suppress p53-mediated transcription.[10,11] *MDM2* expression is positively regulated by p53 transactivation, forming a feedback loop. Amplified *MDM2* has been observed in human sarcomas[9,12] and in >10% of various human cancers including gastric cancers.[13,14] MDM4 was discovered as a p53-binding protein negatively regulated by MDM2 and has structural homology with MDM2.[15] *MDM4* is also amplified or overexpressed in 10–20% of various human cancers[7,16] and 65% of retinoblastomas.[17] Unlike MDM2, MDM4 is neither activated by p53 nor has intrinsic ubiquitin-ligase activity. MDM4 regulates p53 activity by interacting with the p53 transactivation domain and thereby inhibiting p53-mediated gene expression.[18,19]

Nutlin-3 is a novel small-molecule inhibitor of MDM2.[20,21] It binds to MDM2 in the p53-binding pocket, interfering with MDM2-directed p53 degradation and resulting in p53 accumulation. Increased p53 activates p53-responsive genes involved in G_1 arrest and apoptosis. In addition, nutlin-3 exerts antitumor effects in solid tumors and lymphoid neoplasms with wt *p53*.[22–24] However, its *in vitro* and *in vivo* antitumor effects in gastric cancer cells have not yet been sufficiently clarified.

We analyzed various gastric cancer cell lines for the expression of MDM2 and MDM4 and their sensitivity to nutlin-3 with or without anticancer drugs. We also investigated the *in vivo* antitumor effects of nutlin-3 alone and its enhancement by 5-fluorouracil (5-FU) in a xenograft model of a human gastric cancer cell line with wt *p53*.

Materials and Methods

Cell lines. Seven gastric cancer cell lines were used: four cell lines with wt *p53* (MKN-45, NUGC-4, STKM-2, and SNU-1);[25–27] and three cell lines with mutant-type *p53* (mt *p53*; NUGC-3, NUGC-2, and STKM-1).[26] Cell lines with wt *p53* derived from other types of cancer (SJSA-1 osteosarcoma, MCF-7 breast cancer, and Weri-1 retinoblastoma cell lines) were also studied. MKN-45, NUGC-4, and Weri-1 cell lines were obtained from Riken BRC Cell Bank (Tsukuba, Japan). SNU-1, SJSA-1, and WI-38 (human diploid fibroblasts) cell lines were purchased from the American Type Culture Collection (Rockville, MD, USA). NUGC-3 and NUGC-2 cell lines were obtained from Health Science Research Resources Bank (Osaka, Japan). STKM-1 and STKM-2 cell lines were kindly provided by Dr. Shunsuke Yanoma (School of Medicine, Yokohama City University, Japan).

Chemicals. Nutlin-3 and 5-FU were purchased from Calbiochem (San Diego, CA, USA) and Wako (Osaka, Japan), respectively. Cisplatin (CDDP) was obtained from Toronto Research Chemicals (North York, ON, Canada). All reagents were used in different concentrations as indicated.

Immunoblot analysis. Both SDS-PAGE and Western blot analysis were carried out as previously described.[28] Primary and secondary antibodies used were as follows. Monoclonal antibodies against MDM2 (2A10), MDM4 (MDMX-82), $p21^{WAF1}$ (EA10), and Noxa (114C307) were purchased from Abcam (Cambridge, MA, USA). Anti-MDM4 (D-4) antibody was obtained from Santa Cruz Biotechnology (Santa Cruz, CA, USA). Anti-p53 mouse mAb (BP53-12) was purchased from

[3]To whom correspondence should be addressed.
E-mail: ihyodo@md.tsukuba.ac.jp

doi: 10.1111/j.1349-7006.2010.01821.x
© 2011 Japanese Cancer Association

Cell Sciences (Canton, MA, USA). Anti-p14^{ARF} (DCS-240) mouse monoclonal, ALP-conjugated goat anti-mouse IgG, and ALP-conjugated anti-rabbit IgG antibodies were obtained from Sigma-Aldrich (St. Louis, MI, USA). Rabbit anti-cleaved poly (ADP)-ribose polymerase (PARP; Asp214) and anti-β-actin mAbs were procured from Cell Signaling Technology (Danvers, MA, USA).

Real-time quantitative PCR analysis of *MDM2* and *MDM4* gene copy numbers. DNA samples were extracted from cell lysate using a QIAamp DNA mini kit (Qiagen, Germantown, MD, USA) according to the manufacturer's instructions. Real-time quantitative PCR was carried out using a Roche LightCycler 480 Real-Time PCR System (Roche Applied Science, Mannheim, Germany). Primers and TaqMan probe for *MDM2*, *MDM4*, and the reference gene of *MRPL19*[29] were obtained from Applied Biosystems (Foster City, CA, USA; Table 1). Reactions were carried out in triplicate under standard thermocycling conditions using 20 ng genomic DNA, 200 nM primers, 1 μM probes, and LightCycler 480 Probes Master (Roche Applied Science), according to the manufacturer's protocol.

DNA extracted from the cell lines and fibroblasts was analyzed for relative amount of the target gene (*MDM2*, *MDM4*) and reference gene (*MRPL19*) by quantitative real-time PCR. The relative copy number (Q) of *MDM2 versus MRPL19* was calculated using the following equation:[30]

Table 1. Polymerase chain reaction primers and TaqMan probes used in this study

Gene	Sequence
MDM2	
Forward primer	5′-CAGGACATCTTATGGCCTGCTT
Reverse primer	5′-GGGCAGGGCTTATTCCTTTT
Probe	5′-FAM-CATGTGCAAAGAAGCTA
MDM4	
Forward primer	5′-TCCCTGCAACTCAGTGGAATT
Reverse primer	5′-TGAGATGGTCTCTTGGCTTTCA
Probe	5′-FAM-TTGGATTTGGCTCACAGTT
MRPL19	
Forward primer	5′-GCTAAACAGAAGGCTCACCACAA
Reverse primer	5′-CACATTTCTGCAACATCCAG
Probe	5′-FAM-ATCTGGCAGGATTATACT

$$Q = qT/qN,$$

$$qT = V^{T}_{\text{target gene}} \Big/ V^{T}_{\text{reference gene}},$$

$$qN = V^{N}_{\text{target gene}} \Big/ V^{N}_{\text{reference gene}},$$

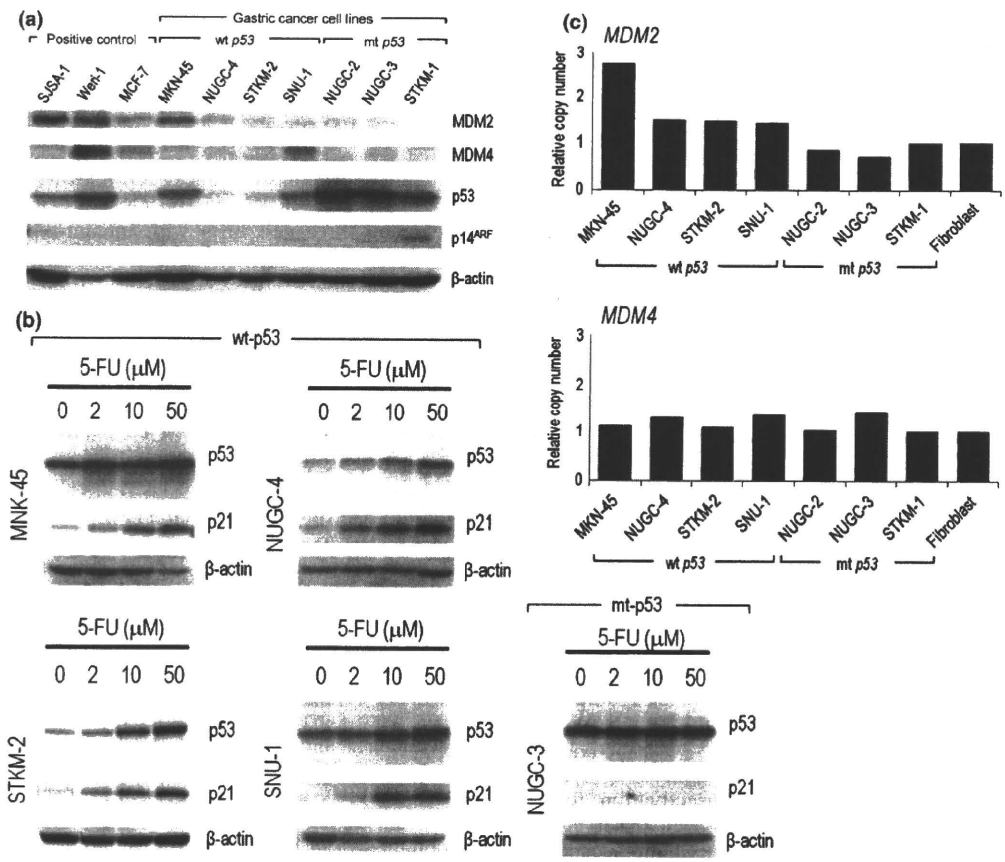

Fig. 1. Expression of human homolog of murine double minute 2 (MDM2), MDM4, and p53 in gastric cancer cells. (a) MDM2, MDM4, p53, and p14^{ARF} expression in seven gastric cancer cell lines was examined by immunoblotting. (b) Four cell lines with wild-type (wt) *p53* (MKN-45, NUGC-4, STKM-2, and SNU-1) and one cell line with mutant-type (mt) *p53* (NUGC-3) were exposed to various concentrations of 5-fluorouracil (5-FU) for 24 h and analyzed for p53 and p21^{WAF1} expression by immunoblotting. (c) DNA amplification of *MDM2* and *MDM4* in gastric cancer cells by quantitative real-time PCR. Copy numbers of *MDM2* and *MDM4* in gastric cancer cell lines were compared with those in fibroblasts using *MRPL19* as a reference gene.

doi: 10.1111/j.1349-7006.2010.01821.x
© 2011 Japanese Cancer Association

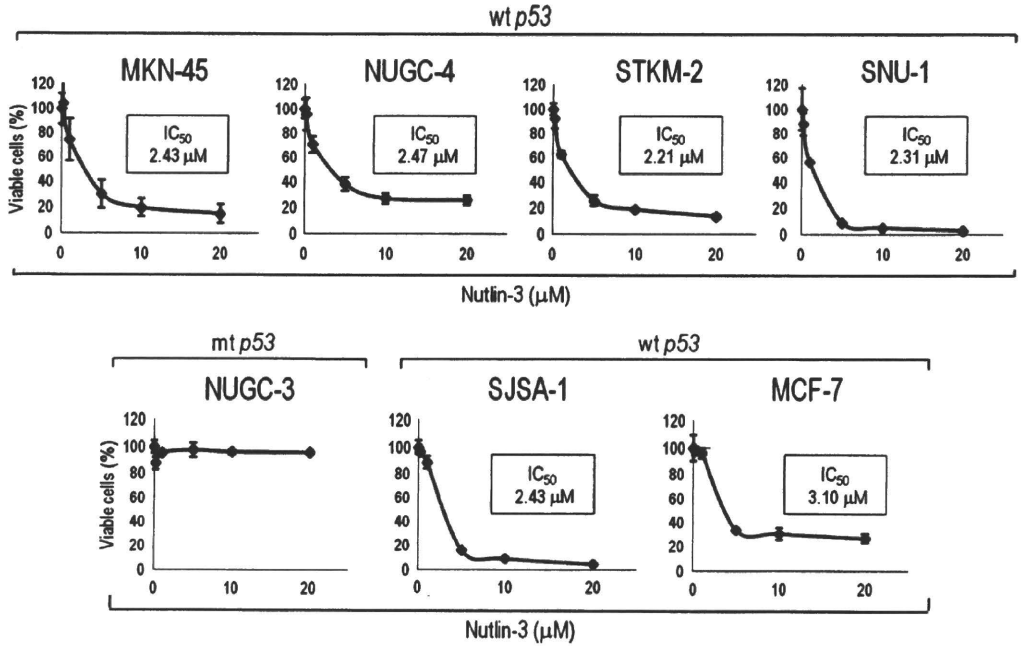

Fig. 2. Nutlin-3 inhibits the growth of gastric cancer cells with wild-type (wt) *p53*. All experiments were carried out in triplicate and the results are expressed as the mean ± SE. mt, mutant-type.

where qT is the ratio of the target gene *versus* the reference gene DNA quantity in the cell line; qN is the ratio of the target gene *versus* the reference gene DNA quantity in fibroblasts: $V^{T}_{\text{target gene}}$ is the relative DNA quantity of the target gene in the cell line; $V^{N}_{\text{target gene}}$ is the relative DNA quantity of the target in fibroblasts; $V_{\text{reference gene}}$ is the relative DNA quantity of the reference gene in the cell line; and $V^{N}_{\text{reference gene}}$ is the relative DNA quantity of the reference gene in fibroblasts.

Cell viability assays. WST-8 colorimetric assays were carried out using a Cell Counting kit-8 (Dojin Laboratories, Kumamoto, Japan) according to the manufacturer's protocol. Cells were seeded into 96-well plates at 5×10^3 cells/well with 100 μL culture medium for 24 h, treated with nutlin-3 and 5-FU for 72 h, then analyzed with an iMark microplate reader (Bio-Rad, Hercules, CA, USA).

Analysis of cell cycle and apoptosis. Cells were seeded into 60-mm dishes at 5×10^5/dish. After incubation with nutlin-3 (10 μM) or an equivalent amount of DMSO for 24 h, cells were gently lifted with Accutase (US Biotechnologies, Parker Ford, PA, USA) at room temperature for 10 min. The cells were then washed once with PBS and stained with a Cycletest Plus DNA reagent kit (BD Biosciences, Franklin Lakes, NJ, USA) according to the manufacturer's protocol. Apoptotic cells were detected by double staining with propidium iodide (PI) and annexin V labeled with FITC using an Annexin V–FITC Apoptosis Detection kit (Beckman Coulter, Brea, CA, USA) according to the manufacturer's protocol. Flow cytometry was carried out using a FACSCalibur flow cytometer and CellQuest software (both BD Biosciences). The percentage of cells in different cell cycle phases was calculated using ModFit LT (Verity Software House, Topsham, ME, USA).

Combination index. To determine whether nutlin-3 can enhance the antitumor effects of conventional chemotherapeutic agents, we used combination index (CI) and an isobologram calculated using CalcuSyn software (Cambridge, UK) according to the Chou and Talalay median effect principle.[31] In this analysis: CI > 1.3 indicates antagonism; CI = 1.1–1.3 moderate antagonism; CI = 0.9–1.1 additive effect; CI = 0.8–0.9 slight synergism; CI = 0.6–0.8 moderate synergism; CI = 0.4–0.6 synergism; and CI = 0.2–0.4 strong synergism.

***In vivo* antitumor effects of nutlin-3 and 5-FU.** Female BALB/c nude mice (5–6 weeks old) were obtained from Charles River Japan (Kanagawa, Japan) and maintained under specific pathogen-free conditions in a temperature and humidity controlled environment. MKN-45 cells were suspended in Hank's balanced salt solution (Sigma-Aldrich), and the cell concentration was adjusted to 5×10^4/μL. Then 100 μL of the adjusted cell suspension of MKN-45 was injected s.c. into the right flank of mice under anesthesia. Ten days later, the s.c. xenografted tumors grew to approximately 5–6 mm in diameter. The mice were randomly assigned to four groups ($n = 6$ per group) as follows: nutlin-3 alone (40 mg/kg), 5-FU alone (40 mg/kg), nutlin-3 (40 mg/kg) plus 5-FU (40 mg/kg), and control (DMSO). Nutlin-3, 5-FU, and DMSO were injected i.p. every 2 days for 2 weeks (six doses). Tumor volume was measured with a caliper twice a week and calculated using $V = \text{length} \times \text{width}^2 \times 0.52$, derived from the formula[32] for the volume of an ellipsoid. To monitor health, the mice were weighed every 2 days and their general physical status was recorded daily.

Statistical analysis. Statistical significance of differences between various groups was evaluated using Dunnett's or Tukey's test. A difference between the experimental groups was considered statistically significant when the P-value was <0.05.

Results

Expression of p53 and molecules regulating p53. MKN-45 cells expressed a high level of MDM2, which was slightly lower than that in SJSA-1 cells (MDM2 positive control). Enhanced MDM4 expression was detected in SNU-1 cells and the MDM4 expression level was intermediate between those in Weri-1 and MCF-7 cells (MDM4 positive controls). The other two cell lines with wt *p53* and three cell lines with mt *p53* did not express

© 2011 Japanese Cancer Association

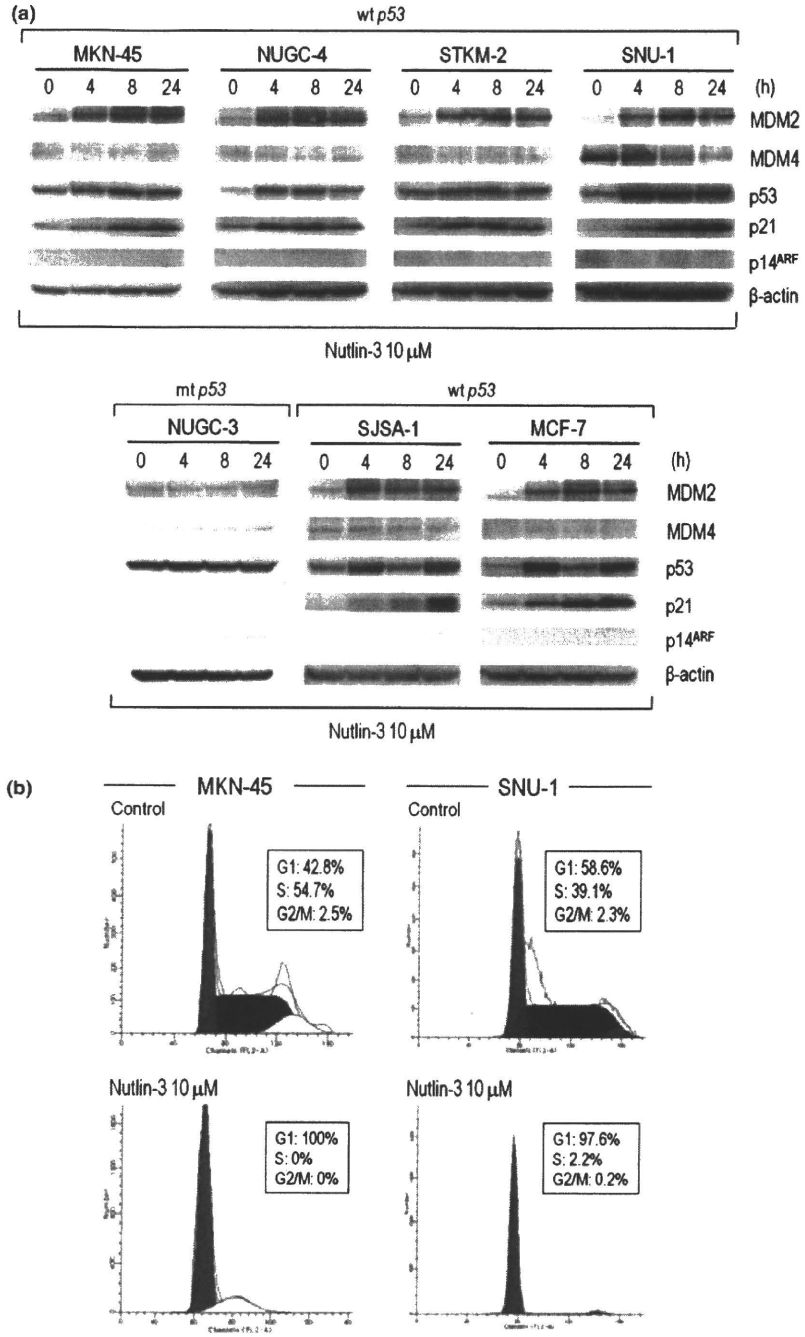

Fig. 3. Effects of nutlin-3 on p53 and $p21^{WAF1}$ expression and cell cycle distribution in gastric cancer cells with wild-type (wt) *p53*. (a) Time-course analysis of the expression of p53 and its downstream molecule $p21^{WAF1}$ in gastric cancer cells treated with nutlin-3. (b) Cell cycle distribution in gastric cancer cell lines with wt *p53* treated with nutlin-3. MDM, human homolog of murine double minute; mt, mutant-type.

either MDM2 or MDM4 at high levels (Fig. 1a). Among the wt *p53* cell lines, SJSA-1, Weri-1, MKN-45, and SNU-1 cells expressed relatively high p53 levels, whereas MCF-7, NUGC-4, and STKM-2 cells expressed lower p53 levels, indicating that the p53 level was positively related to either the MDM2 level or MDM4 level. The cell lines with mt *p53* showed very high p53 levels. $p14^{ARF}$ was detected only in STKM-1. To estimate whether p53 function is intact, four cell lines with wt *p53* (MKN-45, NUGC-4, STKM-2, and SNU-1) and one cell line with mt *p53* (NUGC-3) were exposed to various concentrations of 5-FU for 24 h then analyzed for p53 and $p21^{WAF1}$ levels. All cell lines with wt *p53* accumulated p53 and $p21^{WAF1}$, whereas the cell line with mt *p53* expressed a similar p53 level and undetectable $p21^{WAF1}$ level (Fig. 1b).

Real-time quantitative PCR analysis of *MDM2* and *MDM4* copy numbers in gastric cancer cell lines. Among the cell lines, only MKN-45 cells contained a twofold or higher *MDM2* copy number than fibroblasts. The copy number of *MDM4* in SNU-1 cells was the same as those in fibroblasts and other cell lines with wt *p53*, indicating that MDM4 protein overexpression in SNU-1 cells was not caused by gene amplification (Fig. 1c).

Effects of nutlin-3 on cell growth of gastric cancer cell lines. Gastric cancer cell lines with wt *p53* were cultured in the presence of nutlin-3 (0.2, 1, 5, 10, and 20 μM) for 3 days. A dose-dependent growth suppression was observed in all cell lines with wt *p53*. Their IC_{50} values ranged from 2.21 to 2.47 μM, which were equivalent to those of the MCF-7 and SJSA-1 cell lines (Fig. 2). Nutlin-3 most effectively decreased

doi: 10.1111/j.1349-7006.2010.01821.x
© 2011 Japanese Cancer Association

SNU-1 cell viability (94.8% at 10 μM) compared with the viability of the other cell lines (72.8–81.1%). NUGC-3 cells carrying mt *p53* were resistant to nutlin-3 (IC_{50} = 35.1 μM, data not shown).

Effects of nutlin-3 on expression of p53, MDM2, $p21^{WAF1}$, and MDM4. Both wt *p53* and mt *p53* cells were exposed to nutlin-3 (10 μM) for 0, 4, 8, and 24 h (Fig. 3). Nutlin-3 accumulated p53 as early as 4 h following exposure, with concomitant induction of MDM2 and $p21^{WAF1}$. In SNU-1 cells expressing a high MDM4 level, nutlin-3 inversely decreased MDM4 level. MDM4 expression was hardly detected in the other cell lines with wt *p53*, and nutlin-3 showed no apparent effect on its expression in these cell lines. In the NUGC-3 cell line carrying mt *p53*, nutlin-3 treatment did not increase the MDM2 expression level.

Effects of nutlin-3 on cell cycle in gastric cancer cell lines with wt *p53*. MKN-45 and SNU-1 cell lines were used for examination of cell cycle distribution after incubation with nutlin-3 (10 μM; Fig. 3b). Twenty-four hours after treatment with nutlin-3, the cell fraction of S phase decreased from 54.7% to 0% and the cell fraction of G_1 phase reciprocally increased from 42.8% to 100% in the MKN-45 cell line. Similarly, nutlin-3 exposure decreased the cell fraction of S phase from 39.1% to 2.2% and increased the cell fraction of G_1 phase from 58.6% to 97.6% in the SNU-1 cell line. These results showed that nutlin-3 induced G_1 arrest in these cell lines.

Activation of p53 by nutlin-3 and apoptotic cell death in gastric cancer cells with wt *p53*. MKN-45, NUGC-4, SUN-1, and NUGC-3 cells were exposed to nutlin-3 (10 μM) or an equivalent amount of control vehicle (DMSO) for 72 h, then tumor cells were stained with FITC–annexin V and PI. The cells were analyzed by flow cytometry; cells negative for both annexin V and PI were considered to be non-apoptotic, cells positive for annexin V only were considered to be early apoptotic, and cells positive for both annexin V and PI were considered to be late apoptotic or necrotic. Exposure of MKN-45 cells to nutlin-3 increased the fractions of the early and late phases of apoptosis from 4.6% to 28.4% and from 4.3% to 10.3%, respectively (Fig. 4a). Similar increases in populations of the early and late phases of apoptosis were observed in the other two wt *p53* cell lines (NUGC-4, SNU-1). In contrast, nutlin-3 showed no effects on the population of apoptotic NUGC-3 cells.

Next, the expressions of Noxa, a p53-responsive pro-apoptotic gene product, and cleaved PARP, a marker of caspase 3 activation, were examined in the cell lines with wt *p53* 0, 4, 8, and 24 h after exposure to nutlin-3 (10 μM). The p53 accumulation was detected as early as 4 h after nutlin-3 exposure, and this

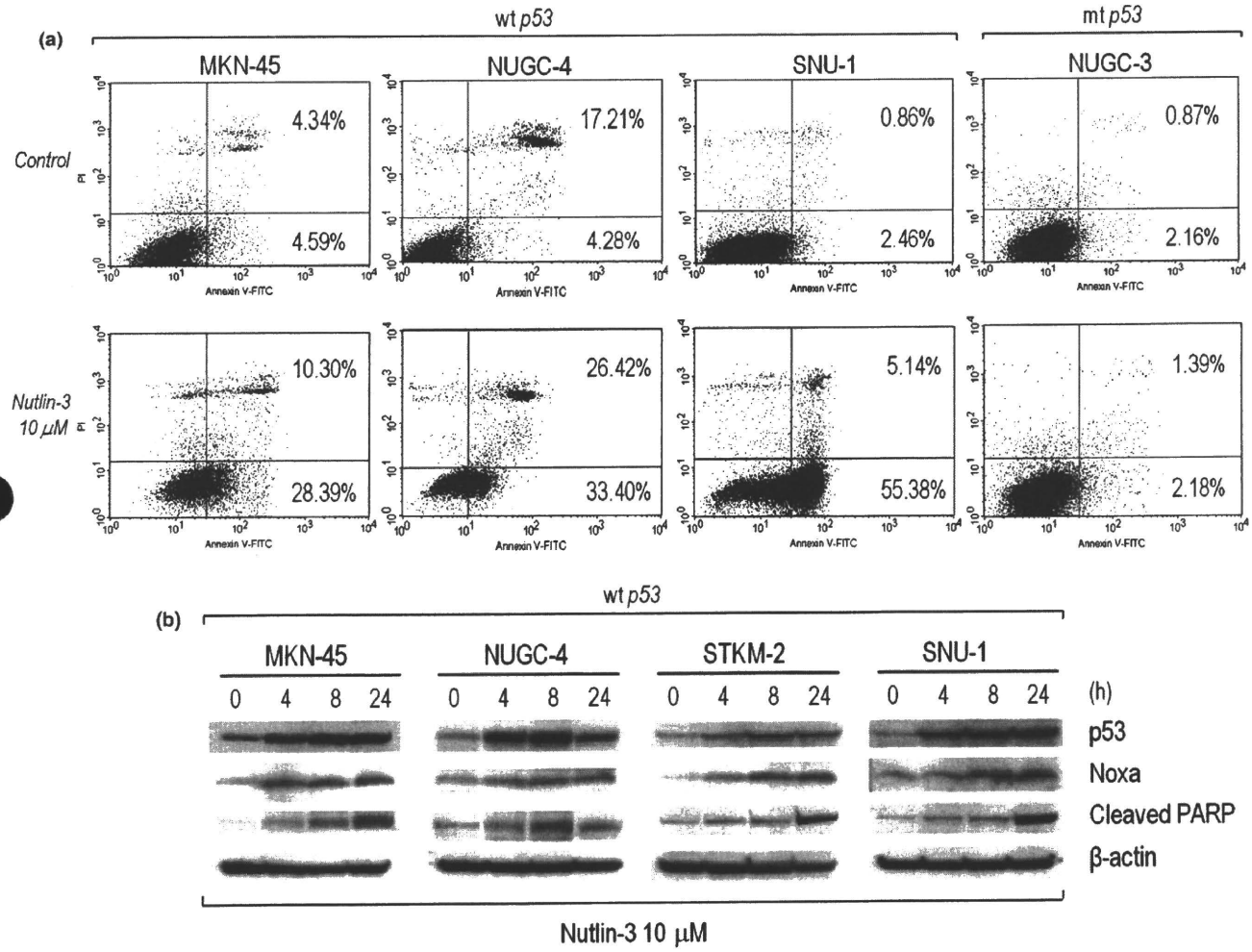

Fig. 4. Induction of apoptotic cell death by nutlin-3 in gastric cancer cell lines with wild-type (wt) *p53*. (a) Detection of apoptotic cell death in gastric cancer cell lines with wt *p53* exposed to nutlin-3. Three cell lines with wt *p53* (MKN-45, NUGC-4, and SNU-1) and one with mutant-type (mt) *p53* (NUGC-3) were treated with nutlin-3 (10 μM) or a vehicle control for 72 h. (b) Effects of nutlin-3 on expression of apoptosis-related proteins (Noxa and cleaved poly (ADP)-ribose polymerase [PARP]) in gastric cancer cell lines with wt *p53*.

© 2011 Japanese Cancer Association

accumulation was accompanied by the expression of Noxa and cleaved PARP in all four cell lines (Fig. 4b).

***In vitro* antitumor effects of 5-FU and CDDP alone or in combination with nutlin-3 in gastric cancer cells with wt *p53*.** We examined whether nutlin-3 can enhance the antitumor effects of conventional chemotherapeutic agents, 5-FU and CDDP, in gastric cancer cell lines with wt *p53*. Specifically, the cell lines with wt *p53* (MKN-45, NUGC-4, STKM-2, and SNU-1) were treated with 0.25 or 1 μM 5-FU alone or 1 μM CDDP alone or in combination with various concentrations (1, 2, and 5 μM) of nutlin-3 (Fig. 5).

The 5-FU and nutlin-3 combination showed an apparent additive effect in MKN-45, STKM-2, and SNU-1 cells but not in NUGC-4 cells. The CDDP and nutlin-3 combination showed an apparent synergistic effect in MKN-45, STKM-2, and SNU-1 cells (Table 2). NUGC-4 cells required a higher concentration of CDDP (5 μM) to achieve a synergistic effect with nutlin-3 than the other three cell lines.

***In vivo* antitumor effects of nutlin-3 alone or in combination with 5-FU.** The *in vivo* antitumor effects of nutlin-3 alone or in combination with 5-FU were analyzed in an MKN-45 xenograft tumor model in nude mice. Injections of nutlin-3 (40 mg/kg, i.p.) or 5-FU (40 mg/kg, i.p.) were well tolerated. No major adverse effects on body weight were observed in the groups of nutlin-3 alone, 5-FU alone, or 5-FU plus nutlin-3 compared with the control group. Both nutlin-3 alone and 5-FU alone significantly inhibited the growth of xenograft tumors compared with the control (Fig. 6a). The combination of these agents showed more potent growth inhibitory effects than did each agent alone.

All mice were killed on day 27, and tumors were excised and weighed. The tumor weights in the nutlin-3 and 5-FU groups were reduced to 58% and 40%, respectively, of that in the control group (Fig. 6b,c). The combination treatment decreased tumor weight to approximately 21% of the control tumor weight, and the weight was significantly less than those in mice treated with nutlin-3 alone or 5-FU alone (Fig. 6b).

Discussion

Mutation or deletion of p53 has been found in approximately 30% of gastric cancers and in approximately 50% of all cancers. This initially suggests that an impaired p53 signal is one of the abnormalities leading to carcinogenesis, and that such impairment might be less important in gastric carcinogenesis. However, abnormalities in genes regulating p53, such as $p14^{ARF}$, *MDM2*, and *MDM4*, as well as abnormalities in downstream genes regulated by p53, have been frequently observed in many

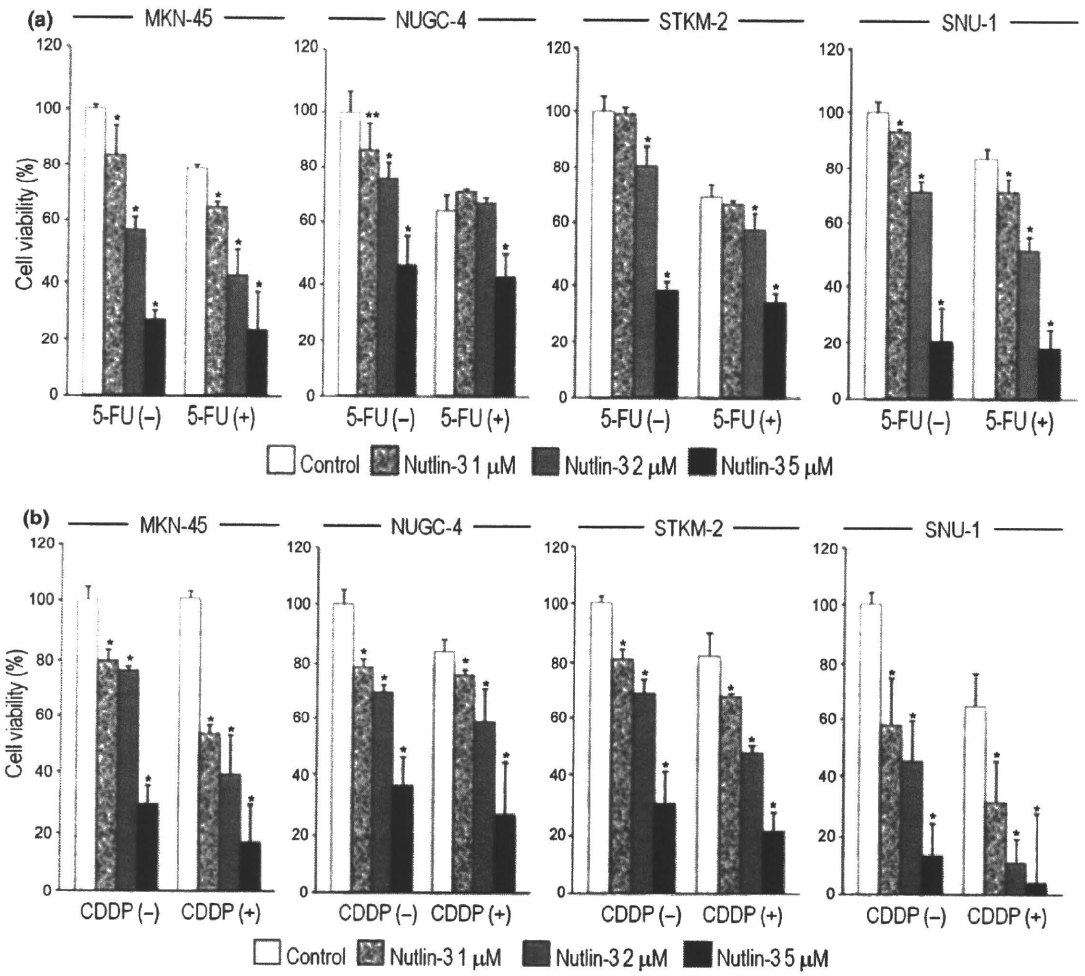

Fig. 5. Cytotoxic effects of chemotherapeutic drugs 5-fluorouracil (5-FU) and cisplatin (CDDP) and enhancement of effects by nutlin-3 in gastric cancer cells with wild-type (wt) *p53*. The cells were cultured for 72 h with the indicated concentrations of nutlin-3 and chemotherapeutic drugs. (a) 5-FU (0.25 or 1 μM) was given in combination with nutlin-3. (b) CDDP (1 μM) was given in combination with nutlin-3. Statistical significance of differences between groups was evaluated using Dunnett's test. $^*P < 0.01$; $^{**}P < 0.05$.

doi: 10.1111/j.1349-7006.2010.01821.x
© 2011 Japanese Cancer Association

Table 2. Combination index (CI) of nutlin-3 plus 5-fluorouracil (5-FU) or cisplatin (CDDP) for gastric cancer cells

Nutlin-3 (μM)	5-FU (μM)	CI			
		MKN-45	NUGC-4	STKM-2	SNU-1
1.00	0.25† or 1.00	1.09	2.21	1.46	1.12
2.00	0.25† or 1.00	0.90	1.56	1.20	1.02
5.00	0.25† or 1.00	0.79	1.49	0.95	0.94
	CDDP (μM)				
1.00	1.00	0.52	1.40	0.83	0.81
2.00	1.00	0.60	0.96	0.62	0.44
5.00	1.00	0.58	0.51	0.53	0.36

†MKN-45 and NUGC-4 cells were treated with 0.25 μM 5-FU. The combined cytotoxic effect of 5-FU or CDDP with nutlin-3 was determined by CI and isobologram. CI > 1.3, antagonism; CI = 1.1–1.3, moderate antagonism; CI = 0.9–1.1, additive effect; CI = 0.8–0.9, slight synergism; CI = 0.6–0.8, moderate synergism; CI = 0.4–0.6, synergism; CI = 0.2–0.4, strong synergism.

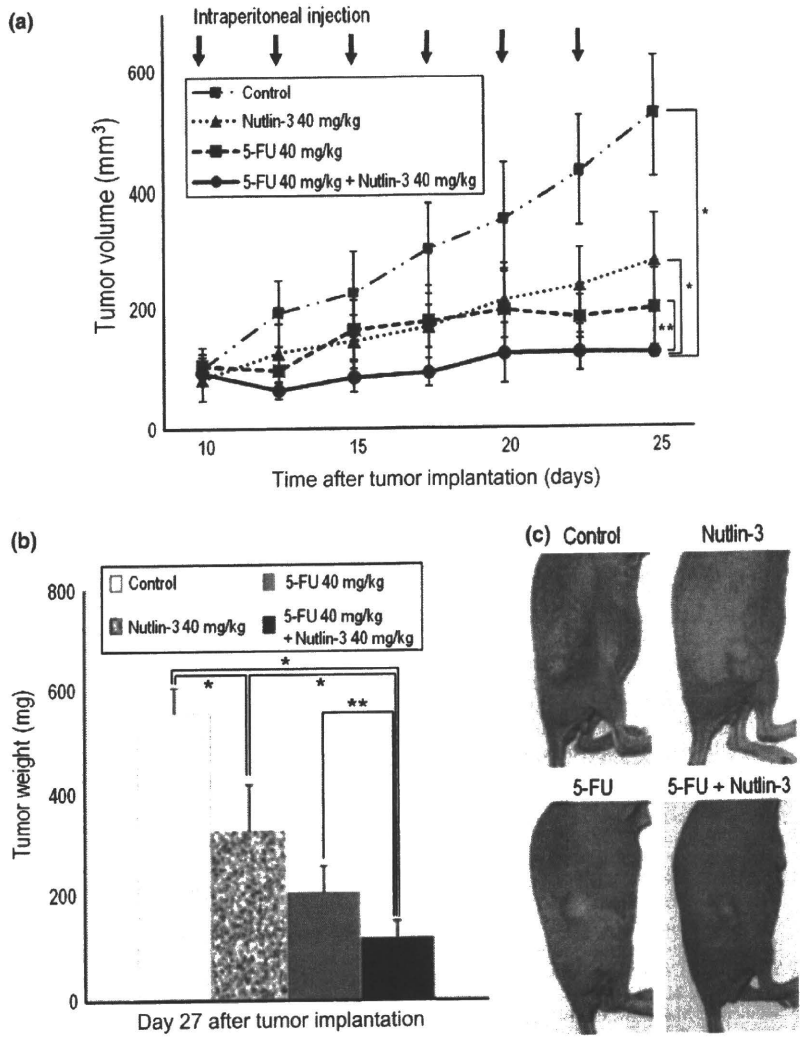

Fig. 6. *In vivo* antitumor activity of nutlin-3 in a xenograft model of a gastric cancer cell line (MKN-45) with wild-type (wt) *p53* and amplified human homolog of murine double minute 2 (*MDM2*). (a) Suppression of *in vivo* growth of MKN-45 cells by nutlin-3, 5-fluorouracil (5-FU), and nutlin-3 plus 5-FU in combination. The results are expressed as the mean ± SE. Statistical significance of differences between groups was evaluated using Dunnett's test. $*P < 0.01$; $**P < 0.05$. (b) Effects of nutlin-3 alone, 5-FU alone, and in combination, on tumor weight. Data are expressed as the mean ± SE. Statistical significance of differences between groups was evaluated using Tukey's test. $*P < 0.01$; $**P < 0.05$. (c) Representative photographs of MKN-45 tumor-bearing BALB/c nude mice treated with either vehicle control or nutlin-3 and 5-FU.

cancer cells. This led to the hypothesis that abnormality in the p53 signal pathway, which is found in almost all cancer cells, is the hallmark of cancers.[33,34] Our results indicating the efficacy of nutlin-3 in all gastric cancer cell lines with wt *p53* (Figs 2–4) are in agreement with those of recent studies investigating nutlin-3 efficacy in other malignancies.[22–24,35,36] Taken together, these results clearly support the above hypothesis that an impaired p53 signal pathway by downregulated p53 plays a critical role in the carcinogenesis of cells with wt *p53*, and the restoration of this p53 signal by nutlin-3 is indeed a very attractive therapeutic strategy for the control of cancers with wt *p53*.

SNU-1 cells with MDM4 overexpression were highly sensitive to treatment with nutlin-3 in our study. Previous studies have shown that other types of cancer cells with overexpression of MDM4 are resistant to nutlin-3.[37–39] The underlying reason for this discrepancy remains unclear. Another study has

© 2011 Japanese Cancer Association

substantiated that MDM4 reduction was caused by MDM2 accumulation as induced by nutlin-3-reactivated p53 in cancer cells overexpressing MDM4.[40] It suggests that this effect was mediated by ubiquitin ligase activity of MDM2. We showed that MDM4 in SUN-1 cells was decreased by the nutlin-3 exposure as the report pointed out, and also confirmed that the proteasome inhibitor MG132 inhibits this MDM4 reduction induced by nutlin-3 (data not shown). Therefore, MDM2 accumulation after nutlin-3 treatment was considered to facilitate MDM4 degradation in SNU-1 cells, and this might result in the susceptibility to nutlin-3 in SNU-1 cells. Another previous report suggested that the K-*Ras* oncogene and insulin-like growth factor 1 induce MDM4 expression through activation of mRNA transcription.[16] These other activation mechanisms of MDM4 might have caused the different sensitivity of MDM4 overexpressed cells to nutlin-3.

Nutlin-3 could not accumulate MDM2 in NUGC-3 cells with mt *p53* even at the high dosage of 40 μM (data not shown). We observed less expression of MDM2 in cells with mt *p53* before the exposure of nutlin-3. This indicates the disruption of normal p53–MDM2 interaction (positive feedback of accumulated p53 to MDM2), and therefore, MDM2 would not increase after nutlin-3 in NUGC-3 cells.

We found that nutlin-3 worked additively with 5-FU and synergistically with CDDP in the gastric cancer cell lines with wt *p53* (Table 2). 5-Fluorouracil and CDDP were selected as combination drugs for nutlin-3 because they are widely used for the treatment of patients with advanced gastric cancers.[41] 5-Fluorouracil is an antimetabolite that inhibits DNA and RNA synthesis, resulting in cell growth inhibition. It was previously reported that 5-FU exerts cytotoxic effects through ribosomal stress, which leads to inhibition of rRNA processing and inhibition of MDM2–p53 interaction.[42–45] This mechanism of p53 activation by 5-FU might be similar to that by nutlin-3, therefore these two drugs might occasionally work competitively, providing a possible explanation as to why the antitumor effect of 5-FU was not always enhanced synergistically by nutlin-3. In contrast, CDDP inhibits DNA function directly by DNA intercalation, resulting in DNA damage and p53 activation.[46] It has recently been reported that nutlin-3 does not diminish CDDP-induced p53 activation.[47] Moreover, proapoptotic responses, including caspase 3 and caspase 7, have been shown to be significantly enhanced with the nutlin-3 and CDDP combination in cancer cells with wt *p53*.[36]

Nutlin-3 induced p53 accumulation, and 5-FU, which is a key drug in clinical chemotherapy for advanced gastric cancer, exerted an additive antitumor effect against MKN-45 *in vitro*. Moreover, no reports have been published indicating the antitumor effects of combined treatment with 5-FU and nutlin-3 in animal experiments. Therefore, we carried out *in vivo* experiments using a xenograft tumor model of the MDM2 overexpressed cell line MKN-45 and found that the antitumor effects of 5-FU plus nutlin-3 were superior to those of either agent alone without major adverse effects, including body weight loss and diarrhea (Fig. 6).

In conclusion, nutlin-3 alone or in combination with conventional anticancer agents is a novel therapeutic strategy for gastric cancer with wt *p53*.

Acknowledgments

This work was supported in part by Grants-in-Aid from the Ministry of Education, Culture, Sports, Science and Technology of Japan (to I.H.), the Japan Society for the Promotion of Science (to K.Y.), and the Ministry of Health Labor and Welfare of Japan (to K.Y.).

Disclosure Statement

The authors have no conflict of interest.

References

1 Teodoro JG, Evans SK, Green MR. Inhibition of tumor angiogenesis by p53: a new role for the guardian of the genome. *J Mol Med* 2007; **85**: 1175–86.
2 Fridman JS, Lowe SW. Control of apoptosis by p53. *Oncogene* 2003; **22**: 9030–40.
3 Vousden KH, Lu X. Live or let die: the cell's response to p53. *Nat Rev Cancer* 2002; **2**: 594–604.
4 Feki A, Irminger-Finger I. Mutational spectrum of p53 mutations in primary breast and ovarian tumors. *Crit Rev Oncol Hematol* 2004; **52**: 103–16.
5 Hjortsberg T, Rubio-Nevado JM, Hamroun D, Claustre M, Béroud C, Soussi T. *The p53 Mutation HandBook v 2*. 2008. [Cited 29 Nov 2010.] Available from URL: http://p53.free.fr/Database/p53_mutation_HB.html
6 Soussi T, Asselain B, Hamroun D *et al.* Meta-analysis of the p53 mutation database for mutant p53 biological activity reveals a methodologic bias in mutation detection. *Clin Cancer Res* 2006; **12**: 62–9.
7 Toledo F, Wahl GM. MDM2 and MDM4: p53 regulators as targets in anticancer therapy. *Int J Biochem Cell Biol* 2007; **39**: 1476–82.
8 Michael D, Oren M. The p53-Mdm2 module and the ubiquitin system. *Semin Cancer Biol* 2003; **13**: 49–58.
9 Momand J, Jung D, Wilczynski S, Niland J. The MDM2 gene amplification database. *Nucleic Acids Res* 1998; **26**: 3453–9.
10 Schuler M, Green DR. Transcription, apoptosis and p53: catch-22. *Trends Genet* 2005; **21**: 182–7.
11 Schuler M, Maurer U, Goldstein JC *et al.* p53 triggers apoptosis in oncogene-expressing fibroblasts by the induction of Noxa and mitochondrial Bax translocation. *Cell Death Differ* 2003; **10**: 451–60.
12 Oliner JD, Kinzler KW, Meltzer PS, George DL, Vogelstein B. Amplification of a gene encoding a p53-associated protein in human sarcomas. *Nature* 1992; **358**: 80–3.
13 Gunther T, Schneider-Stock R, Hackel C *et al.* Mdm2 gene amplification in gastric cancer correlation with expression of Mdm2 protein and p53 alterations. *Mod Pathol* 2000; **13**: 621–6.
14 Sun LP, Jiang NJ, Fu W, Xue YX, Zhao YS. Relationship between gastric cancer and gene amplification of p14 and mdm2. *Ai Zheng* 2004; **23**: 36–9.
15 Marine JC, Dyer MA, Jochemsen AG. MDMX: from bench to bedside. *J Cell Sci* 2007; **120**: 371–8.
16 Gilkes DM, Pan Y, Coppola D, Yeatman T, Reuther GW, Chen J. Regulation of MDMX expression by mitogenic signaling. *Mol Cell Biol* 2008; **28**: 1999–2010.
17 Laurie NA, Donovan SL, Shih CS *et al.* Inactivation of the p53 pathway in retinoblastoma. *Nature* 2006; **444**: 61–6.
18 Stad R, Ramos YF, Little N *et al.* Hdmx stabilizes Mdm2 and p53. *J Biol Chem* 2000; **275**: 28039–44.
19 Stad R, Little NA, Xirodimas DP *et al.* Mdmx stabilizes p53 and Mdm2 via two distinct mechanisms. *EMBO Rep* 2001; **2**: 1029–34.
20 Vassilev LT, Vu BT, Graves B *et al.* In vivo activation of the p53 pathway by small-molecule antagonists of MDM2. *Science* 2004; **303**: 844–8.
21 Vassilev LT. MDM2 inhibitors for cancer therapy. *Trends Mol Med* 2007; **13**: 23–31.
22 Logan IR, McNeill HV, Cook S, Lu X, Lunec J, Robson CN. Analysis of the MDM2 antagonist nutlin-3 in human prostate cancer cells. *Prostate* 2007; **67**: 900–6.
23 Van Maerken T, Speleman F, Vermeulen J *et al.* Small-molecule MDM2 antagonists as a new therapy concept for neuroblastoma. *Cancer Res* 2006; **66**: 9646–55.
24 Drakos E, Thomaides A, Medeiros LJ *et al.* Inhibition of p53-murine double minute 2 interaction by nutlin-3A stabilizes p53 and induces cell cycle arrest and apoptosis in Hodgkin lymphoma. *Clin Cancer Res* 2007; **13**: 3380–7.
25 Yokozaki H. Molecular characteristics of eight gastric cancer cell lines established in Japan. *Pathol Int* 2000; **50**: 767–77.
26 Iida S, Akiyama Y, Nakajima T *et al.* Alterations and hypermethylation of the p14(ARF) gene in gastric cancer. *Int J Cancer* 2000; **87**: 654–8.
27 Kim SY, Kim JE, Lee KW, Lee HJ. *Lactococcus lactis* ssp. lactis inhibits the proliferation of SNU-1 human stomach cancer cells through induction of G0/G1 cell cycle arrest and apoptosis via p53 and p21 expression. *Ann N Y Acad Sci* 2009; **1171**: 270–5.
28 Yamato K, Yamada T, Kizaki M *et al.* New highly potent and specific E6 and E7 siRNAs for treatment of HPV16 positive cervical cancer. *Cancer Gene Ther* 2008; **15**: 140–53.

doi: 10.1111/j.1349-7006.2010.01821.x
© 2011 Japanese Cancer Association

29 Szabo A, Perou CM, Karaca M *et al.* Statistical modeling for selecting housekeeper genes. *Genome Biol* 2004; **5**: R59.
30 Konigshoff M, Wilhelm J, Bohle RM, Pingoud A, Hahn M. HER-2/neu gene copy number quantified by real-time PCR: comparison of gene amplification, heterozygosity, and immunohistochemical status in breast cancer tissue. *Clin Chem* 2003; **49**: 219–29.
31 Chou TC, Talalay P. Quantitative analysis of dose-effect relationships: the combined effects of multiple drugs or enzyme inhibitors. *Adv Enzyme Regul* 1984; **22**: 27–55.
32 Geran R, Greenberg N, MacDonald M, Schumacher A, Abbott B. Protocols for screening chemical agents and natural products against animal tumors and other biological systems. *Cancer Chemother Rep* 1972; **3**: 1–88.
33 Vogelstein B, Lane D, Levine AJ. Surfing the p53 network. *Nature* 2000; **408**: 307–10.
34 Sherr CJ, McCormick F. The RB and p53 pathways in cancer. *Cancer Cell* 2002; **2**: 103–12.
35 Kojima K, Konopleva M, Samudio IJ *et al.* MDM2 antagonists induce p53-dependent apoptosis in AML: implications for leukemia therapy. *Blood* 2005; **106**: 3150–9.
36 Bauer S, Muhlenberg T, Leahy M *et al.* Therapeutic potential of Mdm2 inhibition in malignant germ cell tumours. *Eur Urol* 2009; **57**: 679–87.
37 Wade M, Wong ET, Tang M, Stommel JM, Wahl GM. Hdmx modulates the outcome of p53 activation in human tumor cells. *J Biol Chem* 2006; **281**: 33036–44.
38 Patton JT, Mayo LD, Singhi AD, Gudkov AV, Stark GR, Jackson MW. Levels of HdmX expression dictate the sensitivity of normal and transformed cells to Nutlin-3. *Cancer Res* 2006; **66**: 3169–76.
39 Hu B, Gilkes DM, Farooqi B, Sebti SM, Chen J. MDMX overexpression prevents p53 activation by the MDM2 inhibitor Nutlin. *J Biol Chem* 2006; **281**: 33030–5.
40 Xia M, Knezevic D, Tovar C, Huang B, Heimbrook DC, Vassilev LT. Elevated MDM2 boosts the apoptotic activity of p53-MDM2 binding inhibitors by facilitating MDMX degradation. *Cell Cycle* 2008; **7**: 1604–12.
41 Ajani JA, Rodriguez W, Bodoky G *et al.* Multicenter phase III comparison of cisplatin/S-1 with cisplatin/infusional fluorouracil in advanced gastric or gastroesophageal adenocarcinoma study: the FLAGS trial. *J Clin Oncol* 2010; **28**: 1547–53.
42 Kanamaru R, Kakuta H, Sato T, Ishioka C, Wakui A. The inhibitory effects of 5-fluorouracil on the metabolism of preribosomal and ribosomal RNA in L-1210 cells in vitro. *Cancer Chemother Pharmacol* 1986; **17**: 43–6.
43 Ghoshal K, Jacob ST. Specific inhibition of pre-ribosomal RNA processing in extracts from the lymphosarcoma cells treated with 5-fluorouracil. *Cancer Res* 1994; **54**: 632–6.
44 Bunz F, Hwang PM, Torrance C *et al.* Disruption of p53 in human cancer cells alters the responses to therapeutic agents. *J Clin Invest* 1999; **104**: 263–9.
45 Sun XX, Dai MS, Lu H. 5-fluorouracil activation of p53 involves an MDM2-ribosomal protein interaction. *J Biol Chem* 2007; **282**: 8052–9.
46 Johnson N, Butour J-L, Villani G, Wimmer F, Defais M, Pierson V. Metal antitumor compounds: the mechanism of action of platinum complexes. *Prog Clin Biochem Med* 1989; **10**: 1–24.
47 Barbieri E, Mehta P, Chen Z *et al.* MDM2 inhibition sensitizes neuroblastoma to chemotherapy-induced apoptotic cell death. *Mol Cancer Ther* 2006; **5**: 2358–65.

© 2011 Japanese Cancer Association